POLITECNICO DI TORINO

Collegio di Ingegneria Elettronica, delle Telecomunicazioni e Fisica

Master of Science Degree
Nanotechnologies for ICTs

Master Thesis

EFFECTS OF ARTIFICIAL AND NATURAL WEATHERING ON INTERIOR POLYMERIC COMPONENTS OF VEHICLES

Advisors

Prof. Carlo Ricciardi

....

Dr. Nello Li Pira

....

Candidate

Nasim Ardeshiri

March 2021

Abstract

In this study, I measured and analyzed the solar exposure in the interiors of three different cars, with the goal of determining the relationship between natural and artificial weathering and the degradation of some of the most commonly used polymers in these vehicles, such as PC, PMMA, PP, PS, and PET.

In the first section of this study, a brief summary of the effect of solar irradiation (specifically UV wavelength) on some specific polymers was provided so that we could review some definitions such as irradiance and illuminance. In order to create an artificial solar irradiation some laboratory apparatuses have been implemented in accordance with international standards. For comparing the effects of natural and artificial weathering on different polymers, some optical, morphological and physical characterizations have been carried out such as color measurement, gloss, haze, roughness, and adhesion.

The main objective of the second part was to characterize our samples in terms of optical physical and morphological properties. Spectrophotometer was used for measuring color changes and haze, gloss meter was utilized for measuring gloss, and profilometer and confocal microscope was used for measuring roughness. Adhesion was tested using standard tape which is specified in ISO 2409. Finally, for assessing surface topography of samples I used confocal microscope.

In the results and discussion section, all the data that was obtained from the samples in various conditions of natural and artificial weathering will be compared.

KEYWORDS: Artificial Weathering; Natural weathering; PC; PMMA; PET; ABS; Irradiance; Illuminance; Colour measurement; Gloss; Haze; Optical characterization; Physical Characterization; Topography Analysis; Roughness; Areal field parameters; Confocal microscope; Spectrophotometer; Profilometer.

Acknowledgments

"Learn how to see. Realize that everything connects to everything else"
- Leonardo da Vinci

Table of Contents

Table of Figures

List of Tables

Chapter 1: Introduction and Literature Review

1.1. Introduction

Nanotechnology has already been widely adopted in the automotive industry. This technology is particularly useful in nanocoating, improved fabrics and structural materials, nanofluids and lubricants, tires, as well as preliminary application in smart glass/windows and video display systems. Nano coatings have a wide range of applications in vehicles from interior to exterior. Another advantage of nanotechnology is enhanced resistance to scratches and wear. Polycarbonate, despite its excellent mechanical properties such as high impact strength, toughness, and light weight, found to be difficult to replace for traditional glass due to the weak resistance to scratch, abrasion, and chemicals.

Wear resistance inside the engine is a particular concern. Thus, ceramic nanostructure coatings have been used to enhance metal parts resistance by reducing the scale of size. More recent technological developments in the nanotechnology have brought forth numerous innovative ideas for patents in the auto industry [1].

Polymers are widely used in nearly everywhere these days, particularly in the automotive sector. It is important to quantify the results of any exposure testing program. Customers are typically concerned with the number of changes that their material will undergo during the exposure. Change in some properties, like color or gloss, can be measured with specialized optical measurement instruments. Mechanical testing and morphology analysis can be used to measure changes in the other physical properties.

Automobile manufacturers have relied on new technology for vehicle accessories. which are all made-up of different polymers like Poly Carbonates (PC), Poly Methyl Methacrylate (PMMA), Acrylonitrile-Butadiene-Styrene (ABS), Acrylic, glass, resin etc. Although these components have a wide range of appealing properties, the effect of environmental conditions on the durability and performance of these materials is not fully understood. The durability, performance and rate of deterioration of these products are all significantly influenced by the material composition, as well as the climate conditions to which they are exposed. The degradation of the mechanical and optical properties of the specimen treated under various environmental conditions are a primary concern when recommending such a polymer for interior part of vehicles. The specifications of climate condition which we are using in this study are basically derived based on the data of the climatic conditions of Florida.

Literature available in this field is very rare. The literature review provides instructions on various types of plastic materials used in various applications, as well as their properties, usage, and limited information on changes in properties due to weathering. It also gives a brief in-sight into technical papers and various studies conducted by different authors or Institutions in the field of weathering on plastic materials.

Shamsundara, B. and V, Mannikar. in their study briefly examines the effects of the weathering on the performance and properties of well-known polymers such as PC and PMMA, PET products which are most commonly used materials in automobile sector. The application of accelerated weathering techniques to evaluate the stability of these product materials is also briefly discussed [2].

1.2. Weathering Test

Changes in material properties caused by exposure to the radiant energy of the sun in conjunction with heat and water in its various states, most notably humidity, dew, and rain could result in weathering. Different polymers degrade at different rates in different conditions, or even in the same condition.

Atlas material testing solutions' weathering testing guidebook explains the factors responsible for weathering, such as what is weathering, weathering factors, secondary effects, synergy, climate, weathering measuring factors, and so on. It also explains the different types of weathering tests, such as natural testing and laboratory testing, as well as the procedure, evaluation, etc. which also explains the weathering cycles simulates the different weathering conditions of natural weathering and their standards. This allows researchers to choose the type of testing and simulation cycles [3].

Japanese researchers present findings from a study of six of the most commonly used polymers. These polymers were exposed to the natural weather conditions in four Japanese locations and also subjected to artificial weathering in seven test units [4]. The degradation of PVC, PMMA, ABS in a dew-cycle tester occurs much faster than in other testers. But three other polymers (PS, POM, PE), initially degrade as fast in the dew-cycle tester as they do in other testers and it is only in the last 1000 hours that the degradation of POM and PE is accelerated. This demonstrates that the acceleration factor of the dew cycle weathering apparatus is greater for some materials than for others when compared to natural weathering or other testers. In most cases, the xenon arc Weather-Ometer and the Fadeometer give a lower degradation rate than do any of the four carbon-arc units used in the experiments. Comparison of the microphotographs of surface deterioration of specimens weathered both outdoors and in test equipment shows that the crack pattern of specimens exposed outdoors most closely resembles the crack pattern produced in a xenon arc Weather-Ometer. When specimens weathered in a xenon arc Weather-Ometer are ranked according to their degree of degradation, the order is closer to the rankings of specimens weathered outdoors than it is the ranking of specimens weathered in most of the carbon-arc units.

Ranking by the thickness of the degraded layer demonstrates that, as is well known in practice, PMMA is clearly the superior polymer. Both natural and artificial exposures confirm its stability. PS degrades twice as fast in Naha than it does in Sapporo whereas PE has similar degradation rates in both locations. This is most likely due to the fact that Naha has more rain and humidity than Sapporo and that PE is less affected by exposure to water than is PS.

The first three weathering devices are effective at simulating the degradation that causes color changes outdoors. There is just one exception (PVC). It is difficult to explain why PVC consistently performs worse than PS in artificial weathering devices when it performs much better in natural exposure. Surprisingly, fadeometers, which are supposed to be capable of determining color stability, perform very poorly in this application.

1.2.1. Natural Weathering Test

Natural weathering is the outdoor exposure of materials to unconcentrated sunlight for the purpose of evaluating the effects of environmental factors such as Temperature, Humidity, UV radiation, Solar radiation, Leaf wetness. The exact weather data for a given geographic location are critical for relating laboratory equipment weathering rate to the actual weathering rate.

Many polymeric materials are subjected to changes in mechanical properties, appearance and surface finish due to prolonged exposure to atmospheric conditions. These include UV-light,

temperature, humidity, oxygen, and contamination effects, and such changes may affect the service lifetime of polymeric components. Thus, sufficient knowledge of the ageing behavior of polymers in different environments is of crucial importance [5].

It is impractical to determine the weathering characteristics of materials in all climates around the world. Therefore, benchmark climates chosen for exposure testing are based on their known severity for material weathering and the product's expected market in that country. When choosing suitable climates and sites for weathering tests in that country, the major marketing area of the material should be taken into account.

- ***Temperature***

The effect of temperature on material weathering includes thermal oxidation degradations as well as the acceleration of other weathering reactions. The "rule of thumb" is that increasing the temperature by 10°C doubles the rate of chemical reaction. Furthermore, solar radiation combined with high temperatures equals a faster rate of degradation [6].

- ***Humidity***

Measure of the amount of water in air, that can lead to physical stress. Humidity can have an impact on both indoor and outdoor products. Relative Humidity (RH) is a term used to describe the amount of water that air at a given temperature can hold. Humidity has the ability to change the rate of degradation as well as the mode of degradation [7].

- ***Solar Radiation***

The physics of light covers all important electromagnetic radiation ranges for weathering, including UV, visible, and infrared radiation. Typically expressed in terms of irradiance and wavelength (λ) [7].

- ***Leaf wetness***

Leaf wetness is a meteorological parameter that describes the amount of dew and precipitation that has been left on surfaces. It is used to monitor leaf moisture for agricultural purposes such as fungus and disease control, irrigation system control, fog and dew detection, and early detection of rainfall.

Measurement of leaf wetness is often problematic. Leaf wetness duration (LWD) is a difficult variable to measure and cannot be considered a true atmospheric variable as it is related to structural and optical surface properties and microclimate. However, when available, the use of sensors to measure LWD is a good option, because estimations by empirical or physical models require several meteorological variables and are sometimes too complex. The sensors used to measure LWD are classified into three types: static leaf wetness instruments, which provide only an indication of wet or dry conditions; mechanical leaf wetness instruments, which record the change in sensor length, size, or weight caused by dew deposition; and electronic leaf wetness instruments, which promote a change in sensor impedance [8].

1.2.2. Artificial Weathering Test

Accelerated weathering exposures can provide useful information in shorter time periods, but the stressors (irradiance, heat, humidity) and their intensity levels must be chosen carefully to avoid activation of unrealistic degradation modes and failure mechanisms that are not seen in

real-world conditions [9]. The method of evaluating degradation under these conditions must also be carefully chosen to ensure identification of the same properties that are most likely to be altered by natural exposure.

Laboratory Weathering Testing Methods is with Xenon Arc lamp which can simulate full spectrum of sunlight and Fluorescent UV lamp which is the best simulation of shortwave UV and possibility of water spray.

Numerous research projects have confirmed that properly filtered xenon arc radiation with full control of temperature, humidity, and rain correlates well with natural exposures. [10, 11]

Different SAE and ISO standards define the weathering test protocol for various polymers, textiles, colors, and painting, among other things. These guidelines also define indoor and outdoor weathering, facilities, light sources, etc., as well as the assessment process and specifications. [7].

The SAE J2412 standard process is commonly used for checking the materials of interior parts. A Controlled Irradiance Xenon-Arc Apparatus is used in this accelerated exposure of automotive interior trim components. The xenon long arc simulates UV and visible solar radiation when filtered properly. Irradiance, Panel Temperature, Chamber Air Temperature & Relative Humidity is needed to be controlled. The test method requires a light dark cycle of 3.8 hours followed by 1 hour dark. This loop will be repeated until the test is complete. For dark cycle there is 95% relative humidity (RH) and 50% RH during light cycle. No water spray is required for interior testing as these sections will not be expected to be exposed to rain or dew formation [12]. The effect of UV and humidity on polycarbonate is discussed in the following review.

The effect of weathering, particularly UV, on unstabilized polycarbonate is well understood. Discoloration, embrittlement, and loss of polymer strength are common signs of polycarbonate deterioration. A maximum lifetime of three years was predicted by exposing different commercial PC with different molecular weights and stabilization to either natural or accelerated conditions. [13, 14, 15]

Polycarbonate was exposed to UVA-340 nm fluorescent lamps in a QUV weathering panel chamber. The rate of photodegradation of polycarbonate can be affected by moisture. According to the findings of this study, the degradation detected at 0% RH was more severe. The exact mechanism by which moisture interferes with photodegradation is not known. However, the oxidized layer formed was thicker at 0% compared to 42% RH. The thicker layer of degraded polymer formed at 0% RH interferes more with the path of light than the thinner layer formed at 42% RH, resulting in lower levels of light transmission and increased levels of haze. At room temperature, the absence of humidity promotes the formation of a deeper layer; however, humidity has no negative effect on PC. However, when combined with UV light, it can cause some surface changes [16].

The mechanical properties of ABS, PMMA, and laminated safety glass were maintained with little change during a one-year accelerated weathering simulation. The laminated glass results show that light transmission remains unchanged, and light transmission decrees are not really significant in terms of glass performance. However, it is expected that as these properties are exposed to more weathering, they will undergo significant changes. All materials eventually showed surface effects of ageing, but more testing is needed to determine whether all materials are fit for vehicle components in terms of safety during crash/ impacts, aesthetics, and durability [17].

Correlation of accelerated ageing data with that of outdoor exposure was performed using a comparison of total UV radiation energy (TUVR) required for Polypropylene degradation (PP).

Accelerated ageing was realized in a Q-Sun Xe-1 exposure chamber using a filtered xenon light source and a dry cycle. Weathering was done at the Brno exposure site, which represents the typical mid-European climate. It was discovered that if the TUVR of both types of ageing is to be directly compared, accelerated ageing should be performed at temperatures ranging from 32–36 °C. Under such conditions, the same amount of TUVR energy induces the same extent of polymer deterioration in both types of ageing and may, therefore, be used for a reliable service life-time prediction. Data obtained through accelerated ageing show that the higher the temperature, the less TUVR energy is required for polymer deterioration [18].

The PMMA specimens were subjected to accelerated aging in a closed-loop controlled environmental chamber. The specimens are examined here at 12 and 18 cumulative months of aging. The results showed that the surface roughness had increased, and the data in this study of formulated PMMA is consistent with the chain scission degradation mechanism, in addition to influencing optical properties, the mechanism of chain scission can affect mechanical characteristic [19].

In a recent study the depletion of the UV stabilization in ethylene vinyl acetate (EVA) was observed in indoor accelerated stress testing where high UV flux was present, however, the failure mode was never observed in outdoor deployed specimens. According to the findings of that study, it was concluded that the UV flux of 60 W/m^2 for 300 <λ< 400 nm was appropriate for indoor aging, whereas higher flux (e.g., 180 W/m^2) incorrectly degraded the UVA within the EVA [20]. Given the limitations of indoor weathering, correlation to field degradation of materials is necessary for lifetime estimation with enhanced reliability.

Assessment of Adhesion

The growing needs of the automotive and aerospace industries for better adhesion of components and surface coatings have motivated a strong research momentum in the last decade to understand polymer adhesion. Adhesion is the interatomic and intermolecular interaction at the interface of two surfaces [21]. The attachment of a paint coating to a polymer bumper bar is a common example of an adhesive system used in the automotive industry. Polypropylene is commonly used in the manufacture of such bumper bars; a material exhibiting poor surface adhesive properties in its native state [22].

Many factors influence adhesion. Because of the diversity and interdisciplinary nature of these phenomena, it has been difficult to develop a single theory or mechanism that explains the chemical and physical manifestations of adhesion.

I used the American National Standards Institute (ANSI) to evaluate the adhesion of the polymer substrate's coating film. In this method for cutting the sample, we can use Sharp razor blade, scalpel, knife or other cutting device having a cutting-edge angle between 15 and 30° that will make lattice pattern with either six or eleven cuts in each direction is made in the film to the substrate with straight hard metal, then pressure-sensitive tape is applied over the lattice and then removed, and adhesion is evaluated by comparison with descriptions and illustrations. When the coating of polymers degrades from UV exposure, its ability to protect against corrosion is reduced.

1.3. Optical Characterization of Polymers

During this experimental study I focused on interior of three different cars, "segment A", "segment B", "segment D". In particular, analyzing the solar exposition and optical characterization of internal components. The dashboard, DAB, cluster, radio, gear shift, tunnel,

left and right seats, and doors are the various interior surfaces. The first objective was to compare the spectral irradiance of sunlight inside the car with a filter spectrum that is commonly used for testing the aging of internal components, and the second objective was to assess the relative illuminance of some internal components considering different orientation and position inside the car.

In the first step, the amount of spectral irradiance inside the car with closed windows at three different times was measured. The term "Irradiance" refers to a measurement of radiometric flux per unit area, also known as flux density. Irradiance is usually expressed in W/m2 (watts per square meter).

Spectral Irradiance

Spectral irradiance is the irradiance of a surface per unit frequency or wavelength. Spectral irradiance of a wavelength spectrum is measured in W/m3 or, more commonly, in W/m2 nm.

Illuminance

The term "illuminance" refers to the amount of photometric flux per unit area, also known as visible flux density. Lux is the most common unit of measurement for illuminance (lumens per square meter). In the following for optical characterization of our samples, mostly PC and PMMA but with different suppliers, it means different coating I am going to compare the effect of Natural Weathering and Artificial Weathering on optical properties of samples, like "Color", "Gloss" and "Haze". Polymer optical properties are inextricably linked to our perception of the quality and visual performance of a plastic product. Testing will provide you with insight into how to accelerate development and optimize the life cycle.

1.3.1. Color

Color is one of the most important quality parameters in the plastics processing industry [23]. Particularly in the automotive industry it is difficult to combine different dyed materials such as leather, plastic and wood. Color is a human brain interpretation of visible electromagnetic waves perceived by the eye [24].
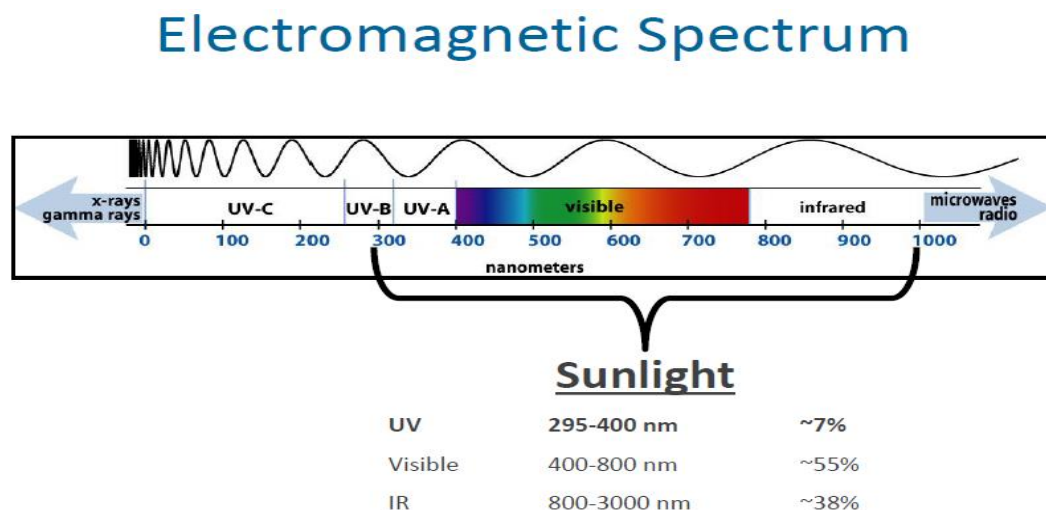
Figure 1.1. Electromagnetic Spectrum

Color measurement is based on the systems published by the Commission International de L'Eclairage (CIE). These systems are based on an understanding of how the human eye and

brain process color information. The CIE Lab represent, in a numerical form, the relevant physical values are determined: lightness (L*), red–greenness (a*) and yellow–blueness (b*) [25]. Many applications of color measurement in the examination of objects require the quantification of color difference, and the shift of an object's color perception depending on the light source is influenced by the combination of colorant and illumination. For this reason, the CIE introduced not only the CIE L*a*b* system but also standardized illuminants. In Europe the standard daylight illuminant (D65) is normally used [26]. There are CIE standards and units for the measurement of color difference. The basic unit of color difference is denoted by the symbol ΔE, which is defined as the distance between two points plotted in CIELab color space.

$$\Delta E_{ab}^* = \sqrt{(L_2^* - L_1^*)^2 + (a_2^* - a_1^*)^2 + (b_2^* - b_1^*)^2}.$$
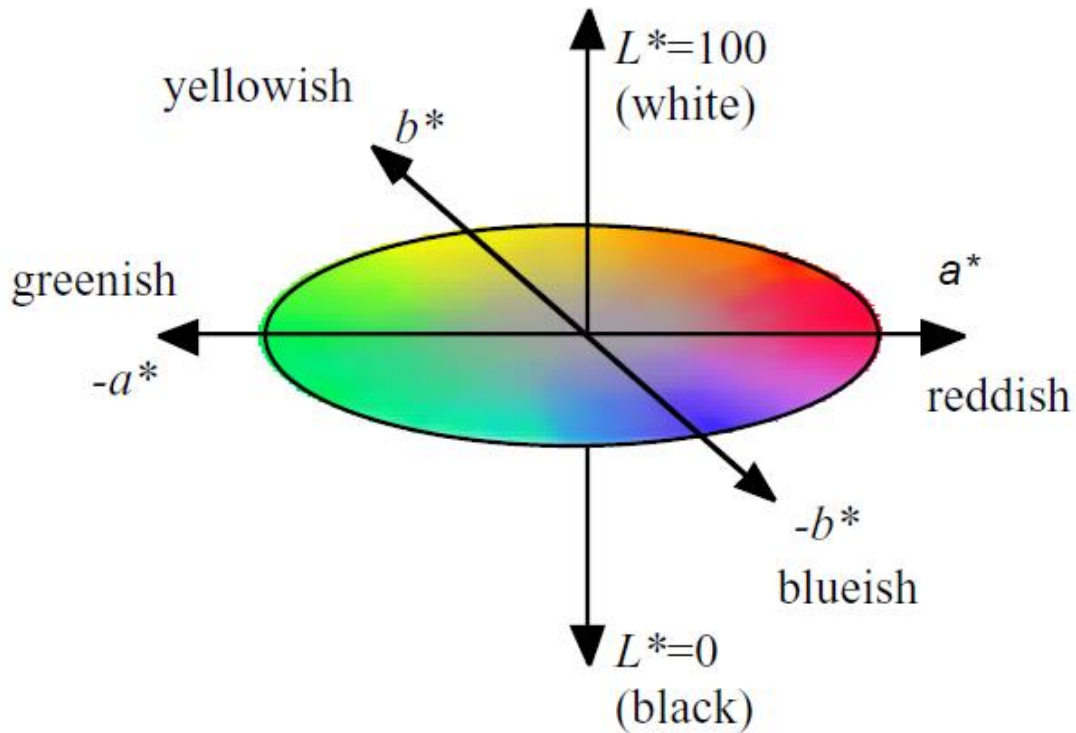
Figure 1.2. CIELab color space

1.3.2. Haze

Within the automotive industry, polymer, plastic or compound materials are tested for their perceptive properties, which describe how a product is perceived by the users regarding to their color, gloss, scratch, haze, appearance and more. I test also the Haze of our transparent samples. According to ASTM D1003-07. "Haze" gives us the percentage of transmitted light that deviates from the incident light beam. Haze can be inherent in the material, a result of the molding process, or a result of surface texture. Haze can also be caused by environmental factors such as weathering or surface abrasion, which results in reduced visibility and/or glare. Light scattering is caused by a variety of factors, including surface roughness and internal optical irregularities caused by crystallization or the level of crystallinity of the material. The level of haze, light transmitting and light scattering properties of transparent materials were

7

measured using spectrophotometers. Haze is primarily caused by hydrolytic degradation in the presence of heat and humidity, and light has little or no effect on its formation [27].

It should be noted that reducing haze does not always result in improved clarity. In many cases, haze caused by surface roughness is inversely related to gloss, another important optical property. The haze increases uninterestingly with increasing roughness [28].

1.3.3. Gloss

Gloss is an optical property that indicates how well a surface reflects light in a specular (mirror-like) direction. It is one of the most important indicators used to describe the visual effect of an object [29]. It has been defined as "the property of surfaces that gives them a shiny or glossy, metallic appearance". A number of factors can have a significant impact on the gloss of a surface, including the angle of incident light and surface topography, the smoothness achieved during polishing, the amount and type of coating applied, and the quality of the substrate [30, 31]. Finding the surface texture of automotive plastics is extremely important from an aesthetic standpoint; additionally, for safety reasons, a plastic surface that is excessively glossy will reflect light and objects to a greater extent and may distract drivers while driving.

This gloss has been extensively used in the coating industry to describe the reflectance properties of a coating. The specular gloss is defined as the ratio of a surface's specular reflectance to the specular intensity reflected by a standard template at an angle of incidence θ:

$$G = 100* (I(\theta))/(I0(\theta))$$

Where I, is the intensity of specular reflection of the sample; I0 is the specular reflectance from the standard template; and θ could be 20°, 60°, or 85° [32].

Manufacturers design their products to be as versatile as possible, from highly reflective car body panels to glossy magazine covers or matt finish automotive interior trim. This is especially noticeable when parts are manufactured by different manufacturers or factories but will be assembled next to one another to form the finished product. Gloss can also be used to assess surface quality; for example, a drop in the gloss of a coated surface may indicate problems with its cure, leading to other failures such as poor adhesion or a lack of protection for the coated surface. A measurement that is proportional to the amount of light reflected by a surface.

The correct measurement geometry should be used according to the sample finish for matt surface 85°, mid gloss: 60° and high gloss 20°. The best angle should be chosen based on the glossiness of the sample surface. The use of the proper measurement geometry improves resolution and the correlation of results with human perception of quality.

Iannuzzi, G. and, Mattsson, B demonstrated that the gloss of the glossy surfaces of the grey specimens of ABS decreased with increasing ageing time. It is also clear that WoM ageing had a significantly greater effect on surface gloss than heat ageing (HA). In fact, the heat ageing had a negligible effect on the gloss. This reduction in gloss would undoubtedly have an effect on the appearance of a component, especially if it was located near another component that was aging at a different rate. The decrease in gloss could be attributed to a slight increase in surface roughness of the specimens as a result of weathering [33].

1.4. Morphological Characterization of Polymers

1.4.1. Roughness

The roughness of the surface is a factor of its texture. It is measured by deviations from the ideal shape of the real surface in the direction of the normal vector. If these deviations are large, the surface is rough; If they are small, the surface is smooth. However, measured (effective) roughness is dependent on the available measurement scale and the sampling interval of the measurement technique. As a result, measured roughness is essentially an extrinsic property. Therefore, the relationship between roughness and measuring length scale remains an unresolved scientific issue. Roughness is an important factor in determining how a real object will interact with its surroundings [34].

In tribology, rough surfaces typically wear out faster and have higher friction rates than smooth surfaces. Because irregularities on the surface can form cracks or corrosion sites, roughness is often a good predictor of mechanical component performance. On the other hand, rough edges can help glue together. Roughness can be measured manually by comparing it to surface coarseness (a sample of known surface roughness), but the surface profile is typically measured using a profilometer. They can be either contact grade (typically a diamond stylus) or optical grade (e.g. white light interferometer or laser scan of a confocal microscope). However, controlled roughness can often be desirable. For example, a glossy surface may be too shiny for the eyes and too slippery for the finger (the touch panel is a good example), so controlled roughness is required. This is the case when both amplitude and frequency are very important.

Specular gloss and surface roughness are important coating factors because they influence the visual perception of a coating on a product [35]. These two parameters, particularly for matt coatings, require more stringent controls [36].

Scientists and technologists anticipate that matt films will have a very low-gloss surface as well as a micro-scale rough surface, which will provide good transparency and a pleasant touch. As a result, many of techniques, such as an additional matting agent [37, 38] and photopolymerization [39, 40] have been widely used to construct rough surface of a coating.

Changes in polymer morphology caused by UV exposure also contributed to an increase in sample surface roughness and a decrease in gloss [41]. The roughness value can be computed on either a profile (line) or a surface (area). To describe a given surface, a variety of roughness parameters can be used [42].
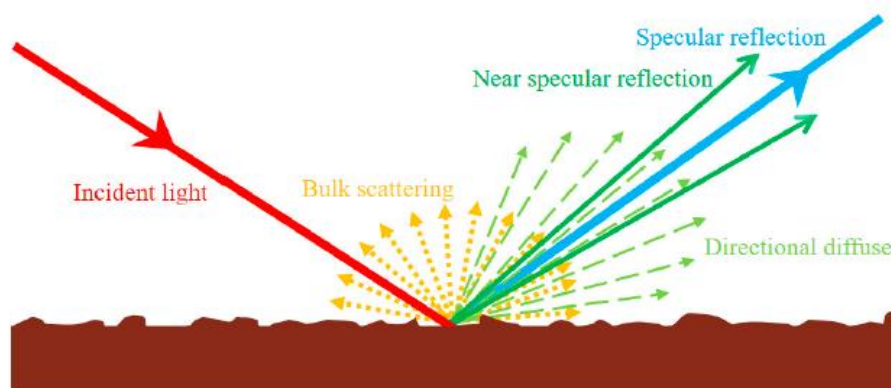
Figure 1.3. A systematic illustration of light scattering at a randomly micro rough surface.

1.4.2. Areal Field Parameter

The field parameters account for the vast majority of surface texture parameters. In contrast to feature parameters, which only take into account specific points, lines, or areas, the term field refers to the use of every data point measured in the evaluation area. Field parameters can be used to characterize surface heights, slopes, complexity, wavelength content, and so on. They are defined in the specification standard ISO 25178 [43].

The most common parameters are calculated from line profiles in accordance with ISO 4287, but due to the increased use of 3D profilers, a set of complementary area roughness parameters has been defined in the ISO 25178 standard [44].

For better understanding of Areal Parameter, the height parameters like Ssk, Sku, Sq and Sa has been selected.

Skewness (Ssk), known as the third moment of the distribution, is used to quantify the level of asymmetry in a distribution. Skewness is negative when there is a great number of large data values causing the distribution to appear to have a long flat tail for smaller values. Conversely, a positive distribution is produced from data dominated by smaller values. A skewness of zero generally indicates that the distribution is symmetric about the mean [45].

$$S_{sk} = \frac{1}{S_q^3} \iint_a (Z(x,y))^3 d(x)dy$$

Kurtosis indicates the level of flatness or sharpness of the distribution. Kurtosis also known as the fourth moment of the distribution, is less than 3 when the distribution has a shorter and flatter peak compared to the ND and is greater than 3 when the distribution has a longer and sharper peak when compared to the ND. Lastly, the kurtosis is equal to 3 for the case of a normal distribution [45].

$$S_{ku} = \frac{1}{S_q^4} \iint_a (Z(x,y))^4 d(x)dy$$

Root Mean Square Height, Sq is defined as the root mean square deviation of the roughness evaluated over the calculated 3D surface [46].

$$S_q = \iint_a (Z(x,y))^2 d(x)dy$$

Arithmetic Mean Height, Sa is defined as the arithmetic mean deviation of the roughness evaluated over the calculated 3D surface [46].

$$S_a = \iint_a |Z(x,y)| d(x)dy$$

The Sa and Sq parameters are highly correlated with one another (Blunt and Jiang2003). The Sq parameter has greater statistical significance (it is the standard deviation) and is often more physically grounded than Sa; for example, Sq is directly related to surface energy and how light is scattered from a surface.

1.5. Polymers and Composites Commonly Used in the Automotive Industry

1.5.1. Poly (ethylene terephthalate), PET

PET, or poly (ethylene terephthalate), is a semi-crystalline thermoplastic polyester that is by far the most widely used polyester. It has the chemical formula [C10H8O4] and a melting point of 260 °C. PET's glass transition temperature ranges between 67 and 81 degrees Celsius. PET polymer is used in the production of a variety of electrical instruments, packaging, X-ray sheets, plastic bottles, and other products. Polyethylene has a homogenous chemical composition and divided into low- and high-density materials with a reference density of 0.94 g/cm3. Each group is highly diverse due to chain irregularities (branches), instaurations, molecular weight variations and components added during the polymerization reaction to influence basic mechanical properties and durability. PET film is widely used in photovoltaic module back sheets due to its dielectric breakdown strength, and in optical displays due to its excellent combination of properties, particularly optical clarity. However, under environmental stressors such as heat, moisture, and ultraviolet irradiance, PET degrades and loses optical clarity. Stabilizers are frequently added to PET formulations to increase durability; however, even these are subject to degradation, reducing optical clarity even further.

The band gap of irradiated PET polymer samples decreased from 3.97eV to 3.88eV with increase of time duration of UV irradiation from 0 to 40 hrs. This indicates that the conductivity of the polymer increases. This decrease in optical band gap could be attributed to increased conjugation as a result of UV-irradiation. This is due to the formation of ion pairs from bond cleavage as energy is imparted to covalent bonds, as well as subsequent processes such as cross linking and chain scissoring, among others. Urbach's energy values in polymers increase with increasing irradiation time and tell about the width of the tail of localized states within the optical band gap. The damage caused by UV irradiation is minor, as evidenced by the shifting of some IR peaks in PET polymer samples [47].

PET film degrades under multifactor accelerated weathering exposures, resulting in haze formation due to high humidity exposures. Neither degradation mechanism was observed during heat and humidity exposures without irradiance [48]. The condition in the Q-Lab QUV weathering chambers (Model QUV/Spray with Solar Eye Irradiance Control) were used for the UV light exposures (HotQUV and CyclicQUV). UVA-340 fluorescent lamps (280–400 nm) are used in the QUV, which closely matches the air mass (AM) 1.5 solar spectrum at wavelengths between 280 and 360 nm. The HotQUV and CyclicQUV exposures had an irradiance of 1.55 W/m2 at 340 nm at 70˚C, comparable to approximately 3 times greater than the intensity of AM 1.5 at 340 nm [49]. The CyclicQUV exposure, per ASTM G154 Cycle 4 standard [50], is a multi-cyclic multi-stressor exposure of alternating sequences of UV light, heat, and condensing humidity designed to mimic outdoor conditions where materials are exposed to morning dew or rain followed by sunlight.

The formation of haze in PET films can be attributed to a variety of factors, including partial crystallinity, or crystallite formation within the bulk material, which can be exacerbated by hydrolysis-induced chain scissions, which increase polymer chain mobility and allow the rearrangement of amorphous polymer chains into ordered crystalline structures. Internal stresses can be caused by volumetric changes in the polymer matrix caused by thermal and/or mechanical expansion and contraction. Internal stresses can cause crazing and cracking in the bulk and/or on the surface, especially as hydrolysis and temperature cycling cause more chain scissions. These stressors can also have an effect on polymer morphology [51].

1.5.2. ABS

ABS, or poly(acrylonitrile–butadiene–styrene), is an amorphous copolymer composed of the thermoplastic copolymer matrix SAN (styrene–acrylonitrile) grafted onto the elastomeric phase PB chains (polybutadiene). ABS is widely used as an engineering polymer (vehicle interiors, domestic appliances, toys, etc.) due to its favorable mechanical properties, which combine the strength and the rigidity of the SAN phase with the toughness of the PB phase, to its good processability and to its relatively low cost. The main disadvantage of using ABS is its limited ageing resistance, particularly in outdoor applications. ABS, in fact, undergoes oxidative degradation when exposed to heat (thermal oxidation), UV-light (photo-oxidation), or mechanical stress in the presence of oxygen [52, 53, 54]. In general, it begins when enough energy is available to activate hydrogen abstraction, resulting in the formation of free radicals [55, 56]. Thus, the polymer's oxidative degradation begins with the formation of free radicals (R, ROO, etc.) that can react with oxygen to produce oxy- and peroxy-radicals, can abstract hydrogen from other polymer chains or react with each other, and participate in a variety of other reactions [55, 57, 58]. Some of these reactions cause chain scission and cross-linking of the rubber component, which degrades the PB phase's elastomeric properties, resulting in mechanical property loss, changes in the chemical structure of the surface regions, and surface discoloration [53, 54, 56, 59]. According to some studies, physical aging of the SAN phase also contributes to surface embrittlement and mechanical property loss [56, 57]. These types of reactions are typically regulated or governed by the availability of oxygen and its ability to penetrate the polymer surface, implying that the effects of ageing are typically confined to the very surface layer of the exposed plastic component [56].

In a study by Iannuzzi, G., Mattsson, B. [60] ABS plaques were subjected to heat ageing and artificial weathering. The first consisted of heat ageing the polymer in an air-circulating oven in accordance with SS- ISO 188 at a constant temperature of 75°C. Samples of uncolored and colored ABS were taken out at different times; 500, 1000, and 1500 h. A heat ageing time of 1500 hours at 75°C corresponds to about 5 years at room temperature. This calculation was made following the Arrhenius model and assuming an activation energy of 60 kJ/mol [61, 62]. The second method of aging made use of an Atlas Weather-Ometer (WoM) model 4000, which generates accelerated weather conditions. The samples were placed in a chamber with a relative humidity of around 50%, and the specimens were irradiated with xenon lamps at wavelengths ranging from 300 to 800 nm. At a wavelength of 420 nm, the light intensity was 1.2 W/m2. The total color DE* caused by ageing was significantly higher in the uncolored ABS specimens than in the gray ones. The artificial weathering resulted in a significantly stronger discoloration, both for the unpigmented and gray specimens. The purpose of this research is to look into the effects of aging on the surface properties of polymers. These components are frequently used in conjunction with other parts made of the same or different plastics. It is then critical that they appear as similar as possible, and that their aging behavior be accurately predicted. If the different polymers do not age at the same rate, they will become increasingly dissimilar over time. This presents a challenge for the design engineer [60].

1.5.3. PMMA

Poly (methyl methacrylate) (PMMA), also known as acrylic, acrylic glass, or plexiglass, and by the trade names Plexiglas, Acrylite, Lucite, Perclax, and Perspex, is a transparent thermoplastic that is frequently used in sheet form as a lightweight or shatter-resistant alternative to glass. It is popular due to its moderate properties, ease of handling and processing, and low cost. Non-modified PMMA is brittle when subjected to load, particularly impact force,

and is more prone to scratching than conventional inorganic glass, but modified PMMA can sometimes achieve high scratch and impact resistance.

PMMA has a glass transition temperature (Tg) of 105 °C. Commercial grades of PMMA have Tg values ranging from 85 to 165 °C; this wide range is due to the large number of commercial compositions that are copolymers with co-monomers other than methyl methacrylate. At room temperature, PMMA is thus an organic glass; that is, it is below its Tg. The forming temperature begins at the glass transition temperature and gradually rises [63].

Due to its refractive index, PMMA transmits up to 92 percent of visible light (3 mm thickness) and reflects about 4 percent of each surface (1.4905 at 589.3 nm). It filters ultraviolet (UV) light with wavelengths shorter than 300 nm (similar to ordinary window glass). To improve absorption in the 300–400 nm range, some manufacturers coat or add additives to PMMA. PMMA transmits infrared light with wavelengths up to 2,800 nm while blocking IR with longer wavelengths up to 25.000 nm. Colored PMMA varieties allow specific IR wavelengths to pass while blocking visible light [64].

When tensile strength, flexural strength, transparency, polish ability, and UV tolerance are more important than impact strength, chemical resistance, and heat resistance, PMMA is a cost-effective alternative to polycarbonate (PC) [65]

In PMMA, two mechanisms of degradation may result in main chain scission: direct main chain scission and ester side chain scission. The following equation describes how direct chain scission works:
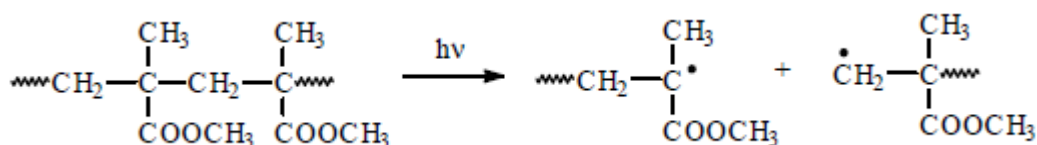
Figure 1.4. Direct chain scission reaction of PMMA

PMMA samples were exposed to monochromatic radiation in the range of 250 to 1000 nm using the Okazaki Large Spectrograph, and the photoirradiated samples were studied using ESR to determine the quantum yield of the main chain scission. A well-resolved nine-line ESR spectrum is produced by direct main chain scission. When exposed to radiation with a wavelength of 300 nm, the above reaction of direct chain scission occurs. As a result, when PMMA is exposed to sunlight, this reaction can occur [66].

Scission of the ester side chain occurs in two steps. The ester group is removed in the first step, resulting in the formation of a radical. This process necessitates more energy than that provided by solar radiation. Radiation at 260 and 280 nm is required for the reaction. Following the formation of the radical, a reaction occurs in which the unsaturated end-group and the radical are formed. The radicals can be oxidized, triggering a series of photooxidative reactions.

The presence of photoinitiators and photo accelerators alters degradation rates and wavelength sensitivity. Pure PMMA must be exposed to radiation with a wavelength less than 320 nm for degradation to occur.

Photochemical changes in PMMA are wavelength specific. In an article by Torikai and Hasegawa [67], they demonstrate that wavelengths less than 320 nm reduce the molecular weight of the polymer. Radiation at 260 and 280 nm is the most effective for chain scission, but exposure to radiation at 300 nm causes relatively large changes. The rate of photolytic degradation slows above 300 nm.

Water exposure causes weight gain. Water has limited compatibility with PMMA, but due to its small molecular size, it will pass through PMMA by Fickean diffusion. The research was carried out in conjunction with environmental stress cracking. Water was discovered to cause the same type of stress cracking as ethylene glycol. Ethylene glycol reduces the weight of the sample. This is due to the fact that ethylene glycol extracts a minor component [68].

Miller in the study of PMMA which was reported after six months of cumulative indoor aging in the environmental chamber equipped with a xenon-arc lamp show. In detail the Specimens were aged in a Ci4000 Weather-Ometer (ATLAS Material Testing Technology LLC), operating at the chamber temperature of 60°C and relative humidity (RH) of 60%, rendering a black-panel temperature of $100 \pm 7°C$. (The local conditions for transparent polymeric specimens were previously verified at 70°C and 38% RH). Specimens were placed in a carousel that rotates about a continuously operating xenon-arc lamp. Borosilicate glass filters were used to filter the lamp so that it closely replicates the AM1.5 spectrum, with the power level being controlled to 114 W·m-2 for $300 \leq \lambda \leq 400$ nm, i.e., 2.5x the AM1.5 global spectrum [69].

Based on the optical flux and duration of exposure (24 hours/day), instruments such as the Ci4000 provide an 8x acceleration factor with respect to the UV dose (with additional acceleration related to the environmental conditions of temperature and RH being location specific). Specimens were aged for cumulative durations of 0, 1, 2, 4, and 6 months, where one month equals 30 days. Because they could not be easily fitted into the standard Ci4000 specimen trays, samples of a domed Fresnel lens (spot-focus) were aged in the dark at 85°C and 85% RH (Blue M FRS-361F, Thermal Product Solutions Corp).

Miller discovered a variation in the optical and mechanical durability of the different specimens. The wavelength at which the specimen began transmitting above -3dB increased from 320 to 615 nm for the most-affected specimen set, with an associated loss in CPV specific photon flux density of 16% and loss in UV optical flux of 90%. The cut-on wavelength remained at 390 nm in the majority of other specimens, with only minor degradation in UV transmittance. In a few cases, the UV bandwidth was increased at a minor cost (0.3% loss) to the CPV specific photon flux, which was attributed to UV stabilization system depletion. Particulate matter accumulated on veteran specimens reduced CPV-specific photon flux and UV optical flux by up to 15% and 29%, respectively. When using multijunction technology, the loss of transmittance at shorter wavelengths with time may eventually result in a current-limited condition at the top cell for soiled as well as optically degraded PMMA.

The yellowness index of the most-affected specimen set increased linearly with time, while loss of mass, another indicator of degradation, increased asymptotically. The average mass loss of 0.7% corresponds to the loss of volatile species caused by photolytic chain scission. Separately, the contact angle was discovered to decrease with age, from 70° in unaged specimens to 50° in old specimens. This means that the specimens will be more easily wetted during aqueous cleaning, but they will also be more prone to soil accumulation. The restoration of contact angle after 6 months of cleaning suggests an accumulation of water-soluble species at the surface. Such species may be formed as a result of the degradation of PMMA and/or its additives. Overt discoloration, crack formation, and hazing were identified during a visual inspection.

In the following Miller shows the specimens are examined at 12 and 18 cumulative months of aging relative to their previously reported condition at 6 months [70].

The samples were stressed in a chamber by exposing them to a combination of ultraviolet (UV) light, temperature, and humidity. The study is intended to aid concentrating photovoltaic (CPV) technology, where a lens made of PMMA is expected to have a lifetime of 25–30 years. Degraded PMMA specimens have been examined using a variety of methods.

The dominant indoor degradation mechanism identified from the methods used for the majority of the formulated PMMA specimens was random chain scission. Gel permeation chromatography was used to directly confirm the mechanism (where a decrease in molecular weight was observed with a negligible increase in polydispersity). The mechanism of chain scission is consistent with the results obtained using indentation (where the modulus was reduced by aging); NMR (where no new peaks were observed, indicating cross-linking or oxidation); and TGA (where the measured activation energy suggests that the mechanism of depolymerization would occur at higher temperatures). Although none of the techniques detected a change in the chemistry of PMMA, NMR could be used to detect changes in copolymers and formulation additives.

Surface morphology (observed erosion/roughening of the surface, as well as the formation of pores and cracks) and X-Ray photo electron spectroscopy (XPS) provided no evidence for the bulk material's degradation mechanism. XPS, on the other hand, suggested the formation of a hydroxyl species at the surface, which may contribute to the mechanism of chain scission.

The additives used in the formulation caused the differences between the ''hazy" and ''yellow" specimen categories. The fluorescence spectroscopy profiles (which investigate the effects of the additives as well as the degraded PMMA material) clearly distinguished between the ''hazy" and ''yellow" specimens. The yellow specimen's optical transmittance profile had changed (relative to a clinical grade specimen with no additives present), indicating that the UV stabilization system had depleted with age.

1.5.4. Polycarbonate, PC

Polycarbonate expressed by general formula:
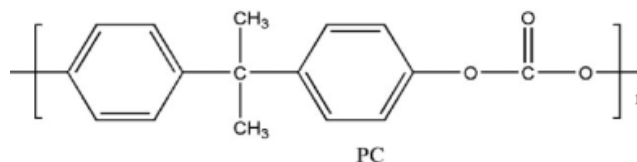
Figure 1.5. Molecular structure of polycarbonate

It can be made from a variety of bifunctional alcohols, but the majority of polymers are made with bisphenol A. Polycarbonate based on bisphenol A is an aromatic compound that can absorb UV radiation from sunlight, making it susceptible to photolytic degradation. UV radiation can cause a variety of changes. The type of change is determined by the wavelength of the radiation. The photo-Fries rearrangement is known to be a step in the degradation of polycarbonates.

Many OEMs in the automotive industry are researching the use of lightweight materials such as PC to produce automotive window glazings. Polymeric glazings are desirable because they can reduce weight by up to 40%–50% and improve fuel economy while providing excellent optics and impact resistance. The injection molding process used for PC enables breakthrough styling for innovative designs as well as cost-effective part integration. Clear silicone hardcoat is applied to the PC substrate to increase its durability. These coatings are used to protect the PC from UV degradation and to provide scratch resistance. Silicone hardcoats can be further improved to resist scratching by deposition of a thin glass-like layer on top of the hardcoat layer using Plasma Enhanced Chemical Vapor Deposition (PECVD), which provides an extremely hard, scratch resistant surface over the hardcoat [71].

Pickett recently investigated the effect of irradiation conditions on the weathering of engineering thermoplastics such as polycarbonate (PC) and PC-ABS blends. The results

showed that samples subjected to shorter wavelengths suffered more damage. Furthermore, for ABS, a nonlinear relationship between irradiance and degradation was discovered [72].

Under the evaluation of polycarbonate after QUV-A radiation in the weathering panel chamber with UVA-340 nm fluorescent lamps. The emission spectra is very similar to that of sunlight for 295 <λ< 340 nm [73]. This radiation was considered suitable for PC, as its activation energy lies in the wavelength range of 290–350 nm, but particularly at λ< 310 nm. The temperature was set at 40 ±2 °C and the RH was either 0% or 42± 5%. UV exposure was continuous for intervals up to 3000 h. The result showed significant increase in haze took place in the UV-aged samples. Samples aged without UV showed less than 1% variation in haze. Whilst under UV, haze increased by about 5.5% in 2500 h of exposure.

Consequently, until 1000 h, specimens exposed to 0% RH developed slightly higher levels of haze than samples aged at 42%, but this was reversed after 1500 h. They noticed a decrease in light transmission as the duration of UV exposure increased. Furthermore, no significant change in light transmission was observed in samples aged without UV at various humidity levels. The reduction in light transmission observed under UV was similar for the two humidity levels: about 5% and 4% for samples aged at 0 and 42% RH, respectively, after 2000 hours of UV. The polymer absorbs more visible light in the blue range as the sample transitions from transparent to yellow, reducing the total light transmitted through the sample.

We know that also moisture can affect the rate of the photodegradation, at 0% RH the degradation detected was more severe. The exact mechanism by which moisture interferes with photodegradation is not known. However, the oxidized layer formed was thicker at 0% compared to 42% RH. The thicker layer of degraded polymer formed at 0% RH interferes more with the path of light than the thinner layer formed at 42% RH, resulting in lower levels of light transmission and increased levels of haze. [74].

For polycarbonate under the condition of mentioned in Tjandraatmadja study [74], Gloss was measured with a Gardner BYK Tri glossmeter at a 60° angle [75]. After 2000 hours of exposure, the level of surface gloss reduction was approximately 5%. As a result, gloss reduction contributes to higher haze levels and a decrease in direct light transmission.

1.5.5. Transparent Coating

Surface engineering is changing the properties of the surface and sub-surface region in a way that's beneficial. Surface modification of materials allows for a variety of advanced properties, such as physical, chemical, electrical, magnetic, optical, mechanical, wear-resistant, corrosion-resistant properties, to be altered on the substrate. The surface chemistry, morphology, and mechanical properties could be important to further adhesion, film formation process and the resulting film properties [76].

Physical vapor deposition (PVD)

Coatings or painting are terms used to describe thick deposits. A coating material is a substance that is applied to other materials to change their surface properties such as color, gloss, wear resistance, or chemical resistance. Paint, varnish, enamel, oils, grease, wax, concrete, lacquer, powder, and metal are examples of coating materials.

PVD techniques are used in a wide range of applications, from decorative to high temperature superconducting films. PVD technologies can deposit a wide range of inorganic materials, including metals, alloys, compounds, and mixtures, as well as some organic materials, such as polymers. PVD is now used to create multilayer coatings, gradient depositions, and extremely thick deposits.

PVD processes employ a variety of vapor phase technologies. In general, PVD refers to a variety of methods for depositing thin solid films onto various surfaces via the condensation of a vaporized form of the solid material. PVD involves the physical ejection of material in the form of atoms or molecules, followed by condensation and nucleation of these atoms onto a substrate. The vapor phase material can be ions or plasma, and it is frequently chemically reacted with gases introduced into the vapor to form new compounds, a process known as reactive deposition. The thicknesses of the deposited layers can range from a few nanometers to thousands of nanometers. [77].

Every PVD process can be defined by three basic steps:

1) Deposition or vapor-phase species generation: material can be converted to a vapor phase via evaporation, sputtering, or chemical vapors and gases.

2) Transport of the species to the substrate: vapor species can be transported from the source to the substrate using line-of-sight, thermal scattering, or molecular flow conditions (without collisions between atoms and molecules). Alternatively, if the partial pressure of the metal vapor and/or gas species in the vapor state is high enough to ionize some of these species (creating a plasma), a large number of collisions will occur in the vapor phase during transport to the substrate.

3) Film deposition on the substrate: after the atoms or molecules have been deposited, the film nucleates on the substrate and grows through a variety of processes. By bombarding the growing film with ions from the vapor phase, the microstructure and composition of the film can be altered, resulting in sputtering and recondensation of the film atoms and enhanced surface mobility of the atoms in the near surface and surface of the film.

All processes are associated with two sets of parameters: plasma, which includes electron density, electron energy, and ion distribution, and process parameters, which include evaporation rate, gas composition, pressure, gas flow rate, substrate bias, and temperature.

Lamination:

Coating and laminating are two of the most common processes for converting flexible films and sheets into finished products. Coating is the application of one or more layers of a fluid or melt to a material's surface, whereas laminating is the bonding of two or more webs. A laminate is any combination of distinctly different plastic film materials or plastic plus non-plastic materials (typically paper and aluminium foil) with each major web being thicker than 6 μm. There is no upper limit to the number of webs that can be used, but two is the obvious minimum, and one of these must be thermoplastic [78]. The primary goal of these treatments is to combine the best qualities of the plastics and substrates.

Transparent Composite:

Because of their novel properties and industrial applications, such as optical fiber sensors, optical isolators, packaging products, and medical devices, optically transparent polymer composites have been the subject of numerous studies in recent years. [79, 80]. According to the ASTM D 1003 standard, the light transmittance, haze, and clarity of PC/SiO2, PMMA/SiO2, PS/SiO2, and PS/Al2O3 composites produced by melt compounding in the Brabender mixer are characterized by light transmittance, haze, and clarity. The degree to which the specimen reduces the apparent contrast of the object is referred to as haze.

The results show that particle content, particle size, and, in particular, the difference in refractive indices between the polymer matrix and the particles have a significant impact on the optical properties of polymer composites. It is also revealed that the light transmittance and

haze of composites are primarily affected by differences in refractive indices, whereas particle size has a greater impact on clarity. Because of their perfect index matching, PMMA/SiO2 nanocomposites have the best optical properties of all composites studied. PC/SiO2 composites exhibit decreased transparency as a result of thermal degradation during the mixing process, as well as a large difference in refractive indices.

Because of better index matching, PS/Al2O3 composites have higher total light transmittance and haze than PS/SiO2 composites, but lower clarity due to larger alumina agglomerates.

Because of increased light loss via reflection and scattering, the haze value of all composites increases with particle concentration. It is worth noting that the haze value of PMMA composites increases only slightly due to perfect index-matching, whereas the haze value of other composites increases dramatically.

Second, Rayleigh light scattering in composites caused by dispersed particles with sizes smaller than the light wavelength used is the primary cause of increased haze (a condition for Rayleigh scattering) [81]. According to SEM analysis, the average size of alumina particles (>10 nm) is much larger than the light wavelength (589 nm), whereas the average size of silica nanoparticles (about 80 nm) is much smaller. As a result, Rayleigh scattering is much weaker in PS/Al2O3 composites than in PS/SiO2 composites. Because of thermal degradation of the PC matrix and large fluctuations in refractive indices, haze values in PC/SiO2 composites are obviously higher than in other composites.

Surface analysis in this work revealed that the outer surfaces of the respective samples are smooth, with an average surface roughness of less than 1 µm. Surface roughness in the 100-lm size range is known to cause a loss in transparency, whereas surface roughness in the submicron range has no effect on transparency [82].

Chapter 2: Materials and Experimental Methods

In this chapter, the raw materials and characterization techniques will be presented, as well as the data on the samples, which will be presented in the table below. Samples A, B, D, E, G, H, and I were analyzed in two separate conditions: Transparent interiors are used in applications such as clusters, radios, and displays, whereas black interiors are used in applications such as dashboards, doors, and seats. The two sample examples, K and L, were used for radio display inside segments A and B. Furthermore, the M, N, and P were only available in black for research purposes.

I didn't bring up the segment for other optical surfaces because those surfaces were being investigated for future research (*).

Table 2.1. Specification of samples

Optical Surface	Substrate	Optical finishing	Segment
Sample A	PC	Matt	*
Sample B	PC	Matt	*
Sample D	PC	Matt	*
Sample E	PC	Gloss	*
Sample G	PC	Matt	D
Sample H	PC/PMMA laminated	Gloss	*
Sample I	PC/PMMA laminated	Gloss	*
Sample K	PC	Anti-Glare	A & B
Sample L	PC	Anti-Glare	B
Sample M	PC	High gloss	*
Sample N	PC	Anti-Glare	*
Sample P	PC	Matt	*

2.1. Characterization Techniques

2.1.1. Spectral irradiance measurement (ILT-950)

There are various instruments for measuring light, such as radiometers, photometers, optometers, dataloggers, lux meters, chroma meters, spectrometers, and spectroradiometers. These meters are intended for measuring light in the infrared, near-infrared, visible, and ultraviolet ranges. The ILT950 remote optic irradiance spectroradiometer system detects spectral ranges from 250 to 1050 nm.

Spectroradiometer system with integrated spheres, cosine correcting diffusers, fiber patch cords, and our complimentary Spectrilight III software for easy and accurate measurement of spectral irradiance, as well as photometry, color coordinates, CCT, illumination, peak wavelength, and more.

High performance, precision, ease of use, and a wide range of features are combined in a rugged, compact, portable design. The ILT950 spectroradiometer's excellent performance was further enhanced by the addition of a new technologically advanced CMOS linear image sensor. The new sensor has a more balanced overall spectral sensitivity (consistent in UV and lower in VIS and NIR), a faster response time, faster data transfer rates, and a wider range of integration times (30 µs to 59 s), all of which increase the overall dynamic range. The ILT950 spectroradiometer light measurement systems are available in two models: broad band (200-1100 nm) and UV (200-450 nm). ILT systems are pre-configured.

Figure 2.1. Spectroradiometer ILT 950

2.1.2. Illuminance measurement (Konica Minolta CL-200A)

The T-10A is the illuminance meter of choice for evaluating light illumination at a specific location or performing lux measurements. On the LCD screen of this advanced lux meter, the illumination and average measurement values will be displayed quickly. The illuminance values can be easily compared and displayed as a percentage or a difference value.

The T-10A is simple to program; the target level can be entered by taking actual measurements or by typing it on the handy keypad. This instrument's high versatility allows it to measure both intermittent and continuous light sources, and it automatically calibrates the moment it is turned on. Even inexperienced users will find it simple to enter color correction factors that can be used to measure any type of light source.

The T-10A lux meter is one of the most useful and functional on the market today. This instrument provides extremely accurate results for tasks involving the measurement of pulse width modification of controlled light sources due to its wide measurement range of 0.01 to 299,000 lx and the ability to switch ranges automatically. If you are measuring multiple sources, you can easily remove the receiver instruments' heads to simplify the process.
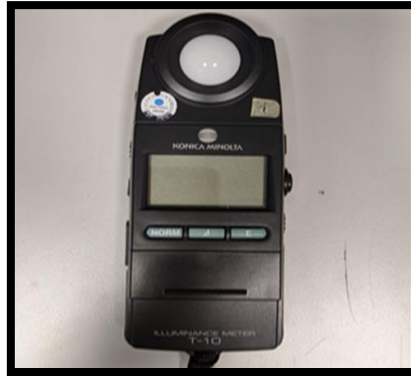
Figure 2.2. Illuminance meter-Konica Minolta CL-200A

2.1.3. Spectrophotometer

The basic idea behind spectroscopic analysis is to send light of a known wavelength through a sample and measure how much light is absorbed or reflected. As a result, the spectrophotometer must be capable of producing discrete wavelengths of light and passing them through the sample.

Spectrophotometers work in addition to the previous process by reflecting light from the surface and recording the wavelength distribution of the reflected light. A polychromatic light source illuminates the sample, and the reflected light is recorded as spectral data by a detector. The spectral data can be used to calculate and convert values to a variety of three-dimensional color spaces. To ensure that it has occurred, the data presented in this work is provided in the color space of CIE L*a*b*.

Specular reflection occurs when light reflects at an equal but opposite angle from the light source; this reflection is especially noticeable on objects with glossy smooth surfaces. Diffuse reflection occurs when the reflected light is scattered in many directions, and it is most noticeable on objects with a matt or irregular surface.

The Specular Component Included (SCI) measurement mode is preferred for measuring an object's true color without the influence of surface conditions. SCI mode incorporates both specular and diffused reflected light and is ideal for computer color matching and color quality monitoring.

The Specular Component Excluded (SCE) measurement mode, which excludes specular reflected light, is used to assess an object's color, which correlates to visual perception. In SCE mode, a glossy surface will typically measure darker than a matt surface of the same color; this corresponds to how our eyes perceive it. This mode is typically used during quality control evaluations to ensure that color meets color standards through visual inspection.
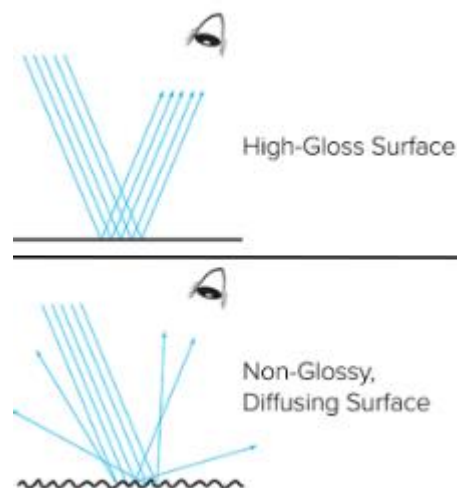
Figure 2.3. Surface condition

2.1.4. Spectrophotometer KONICA MINOLTA CM-3610A

The CM-3610A Spectrophotometer is a high-precision, high-reliability bench-top instrument with vertical alignment that can measure colors in reflectance (diffused illumination, 8-degree viewing) or transmittance (diffused illumination, 0-degree viewing). The detector is a Silicon photodiode array, the spectral separation device is a diffraction grating, and the wavelength range is 360 to Which reflectance mode is best for black samples and which transmittance mode is best for transparent ones? Furthermore, the Spectra Magic software attempted to use SCE for all parameters when calculating color changes due to weathering (L, a, b).

Light from the pulsed xenon lamps is diffused by reflection from the inner surface of the integrating sphere and the surface of the white calibration plate covering the reflectance measurement aperture, and then illuminates the specimen in the transmittance chamber, where it is received by the specimen- measuring optical system and guided to the sensor, then the light from the specimen-measuring and illumination-monitoring optical fibers is then divided into wavelength components and projected onto the sensor array section, which converts the light into proportional currents and outputs the currents to the analog processing circuit.

Calculating the Haze(D1003-97) (A) with the CM-3610A is extremely simple, and haze has been estimated using the transmittance mode for all transparent samples. The measurement geometry for transmittance measurements becomes di:0° (diffused illumination) when the White Calibration Plate is placed over the reflectance measuring aperture. As a result, haze has a wide range of applications, including plastics, textiles, paints, ceramics, and so on.

This Optical System technology can handle measurements for numerical gloss control (NGC) for simultaneous measurements with specular component included (SCI) and specular component excluded (SCI) (SCE). Furthermore, numerical UV control (NUVC) is the leading technology for UV adjustments to measure samples containing optical brighteners such as paper textiles, pulp, or other chemicals.

These technologies ensure the highest levels of repeatability and accuracy. The CM-3610A has superior reliability and an incredible price-performance ratio thanks to its low number of moving parts.

Spectra Magic is a color measurement software package that can be used to interface with Konica Minolta instruments and provide extended color and color difference reporting and analysis. The CM-3610A can measure both the reflectance of opaque objects and the transmittance of solid materials that are transparent or translucent, such as plastics.

Figure 2.4. Spectrophotometer KONICA MINOLTA CM-3610A

2.1.5. Varian spectrophotometer Cary 500 UV-Vis-NIR

Spectral photometry is a device that measures the intensity of each color's wavelength. Spectrometers use dispersive elements such as gratings to disperse light at different wavelengths (diffractive elements). Image sensors and other devices detect the dispersed light.

The Cary 500 allows you to control the parameters in the UV-Vis and NIR regions independently, so you don't have to compromise when scanning across the entire range. If you want more detail in the NIR without sacrificing measurement time, simply set a narrow SBW and small data interval in the NIR and a wider SBW and larger data interval (and thus a faster scan speed) in the UV-Vis. This is a measure of the amount of light that is selectively absorbed by molecules within a substance in UV-Vis NIR spectrophotometry. The absorption in the sample is proportional to the distance traveled by the light through the sample. It is also affected by the wavelength of the incident light, as different combinations of molecules absorb different wavelengths. The peaks formed by the various absorption peaks allow for sample characterization and quantitative analysis.

With this instrument, I measured the HAZE of our samples, which tells us the percentage of scattered light that was transmitted, in the middle of the visible range at 550 nm.

Figure 2.5. Varian spectrophotometer Cary 500 UV-Vis-NIR

2.1.6. Veeco DEKTAK 150 Profilometer

Veeco Dektak 150 is a surface profilometer that measures two-dimensional surface profiles using contact profilometry techniques. The Dektak 150 employs a stylus with a low inertia sensor. A sharp probe tip is scanned across a material in a linear fashion to create a height vs distance line profile. It can be used to measure surface topography, roughness, and step heights.

The Dektak 150 can be outfitted with a 150-millimeter X-Y auto stage for 3D mapping, automation, and programmability of up to 200 sample sites. It can also be outfitted with a 6-inch square, porous chuck for photovoltaic applications. The Dektak 150's innovative design allows it to scan samples up to 90 millimeters thick, performs long scans of 55 millimeters, and has a larger X-Y translation than competing systems.

The Dektak 150 option provides the flexibility to perform precise step-height measurements for thin films down to 10 angstroms, as well as thick-film measurements up to several hundred microns thick, with 4-angstrom step-height repeatability using optional ultra-low-noise electronics. The Low-Inertia Sensor 3 (LIS 3) head incorporates critical technological advancements to provide extremely accurate measurements with unprecedented sensitivity.

The system's standard vertical range of 1 millimeter, combined with up to 120,000 data points per scan, provides exceptional capability. All of these features combine to provide exceptional horizontal and vertical resolution, allowing for precise planarity scans to measure radius of curvature, flatness, and waviness, as well as characterize thin-film stress on wafers.
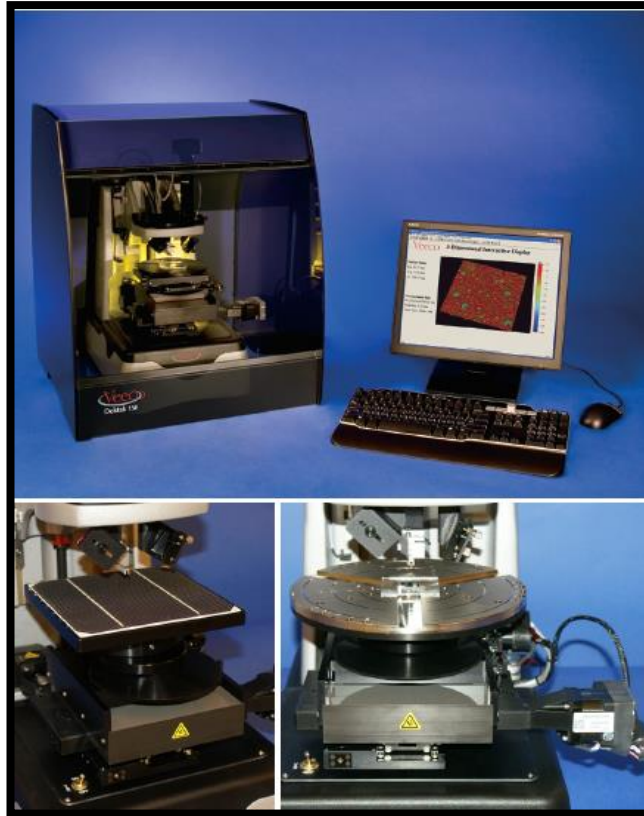
Figure 2.6. Veeco DEKTAK 150 Profilometer

2.1.7. Gloss meter

The Rhopoint IQ quantifies surface quality issues that a standard glossmeter cannot detect and profiles how light is reflected from a surface. This cutting-edge instrument measures: 20/60° Gloss, Haze, Reflected image quality (RIQ), and Image Distinctness (DOI).

The Rhopoint IQ differs from a gloss meter in that it measures the distribution of reflected light between 12.75°–27.25° using a linear diode array (LDA) at 20°. The instrument, unlike a conventional gloss meter, does not have physical receiver apertures; the 20° gloss value is obtained by measuring with the elements of the linear array that correspond to the angles specified in the standards. At 60° and 85°, conventional glossmeter optics are used, which fully comply with international gloss standards such as ISO 2813 and ASTM 523. On the surface, we can see gloss units for 20° and 60°; however, if the number of gloss units exceeds 70, we must consider gloss unit of 20°.

Figure 2.7. Gloss meter-Rhopoint IQ

2.1.8. Confocal Microscope

A confocal microscope can be used to characterize nanoscale surface deformation in the early stages of physical degradation. The Leica DCM8 combines the benefits of HD confocal microscopy and interferometry with a plethora of additional features that enable accurate and reproducible characterization of multiple material surfaces. The sample is scanned vertically at the touch of a button, so that every point on the surface passes through the focus. Within seconds, the Leica DCM8 acquires multiple confocal images at various vertical points along the depth of focus of the objective, automatically adjusting illumination as needed. Out-of-focus data is then removed, and a detailed profile of the surface topography is generated.

We can obtain HD Imaging, HD 3D Topography, Profiles, Coordinates, Thickness, Roughness, Volume, Surface Texture, Spectral Analysis, and Color Analysis with the Leica DCM8. LED light sources provide illumination in the following wavelengths: red (630 nm), green (530 nm), blue (460 nm), and white. A simple image is captured with high lateral resolution using brightfield and darkfield.

Figure 2.8. Confocal Microscope-Leica DCM8

Chapter 3: Results and Discussion

In this chapter, the optical, physical and topographical characteristics of the samples will be discussed.

3.1. Comparison weather data between Florida and Genova

In this study, I compared weather data of Florida site and Genova such as temperature, humidity, solar radiation, UV radiation and leaf wetness which are the influencing parameter in natural weathering. All the data originally were measured on daily basis but for facilitating of analysis, I used the monthly average. The ratio of weathering parameters between these two cities is a simple indicator of how similar these parameters are. The closer this ratio is to one, the more similar they are.

The UV radiation ratio of Genova to Florida is $UV_{Genova}/UV_{Florida}=0.88$

The Solar radiation ratio of Genova to Florida is $SR_{Genova}/SR_{Florida}=0.79$

The Leaf wetness ratio of Genova to Florida is $LW_{Genova}/LW_{Florida}=0.41$

In the first five months and the last three months of the year, the average temperature in Florida is about 10°C higher than in Genova, while the difference is less than 5°C in June, July, and August. The maximum difference in average humidity is approximately 33% in January, and the minimum difference is approximately 5% in November.

3.2. Irradiance

In this analysis I present the measurement of spectral irradiance and illuminance for three different segments (A-B-D). Two objectives have been followed, the first objective was to compare spectral irradiance of sunlight inside the car with filter spectrum which is commonly used for testing aging of the internal components and the second goal was the assessment of the relative illuminance between some internal components with considering the different orientation and the different position inside the car.

For measuring Spectral of irradiance, the calibrated ILT-950 spectroradiometer has been utilized for measuring of "segment A" on 21st June 2018 inside the car with close windows at three different times. As it can be seen, different spectral of irradiance is due to the clear weather condition.

Solar irradiation
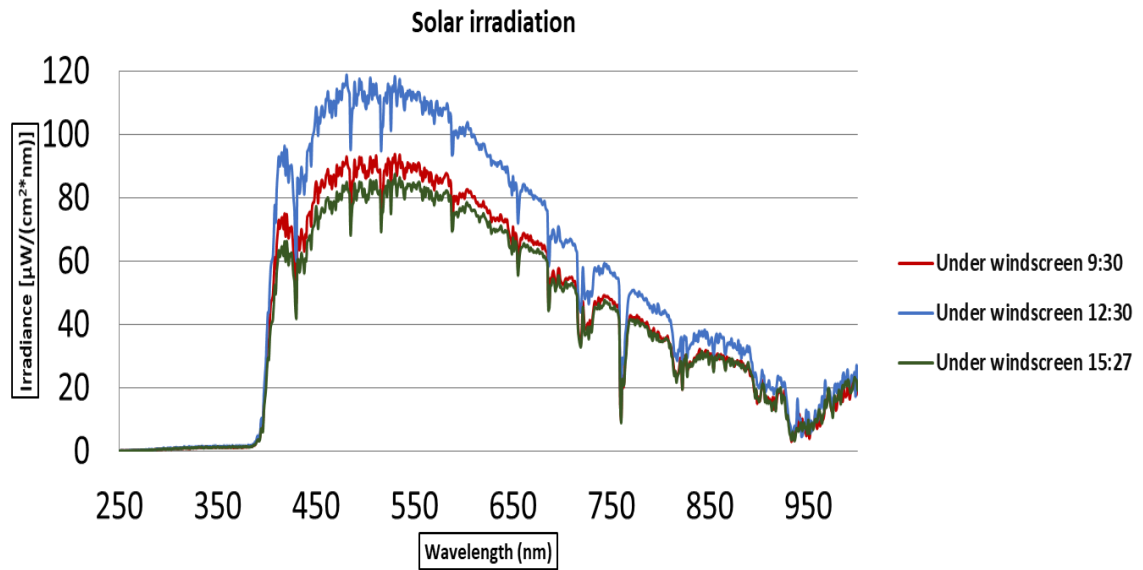
Figure 3.1. Irradiance-Segment A

For "segment B" the measurements were performed inside the car with close windows at three different times on 19th June 2020. As you can see in the **graph 3.2** again the different spectral of irradiance is referred to the clear weather condition.

Solar irradiation
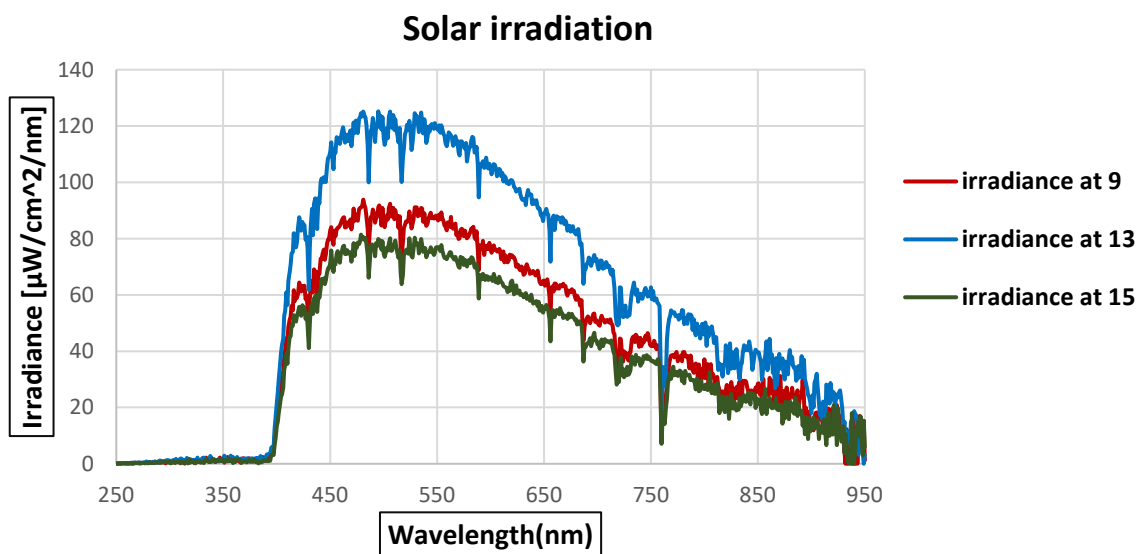
Figure 3.2. Irradiance-Segment B

The measurement of the spectral irradiance for "segment D" was carried out on 5th June 2020 at three different time with close windows. Overlapping of the irradiance at 9 AM and 13 PM is due to the cloudy weather condition.
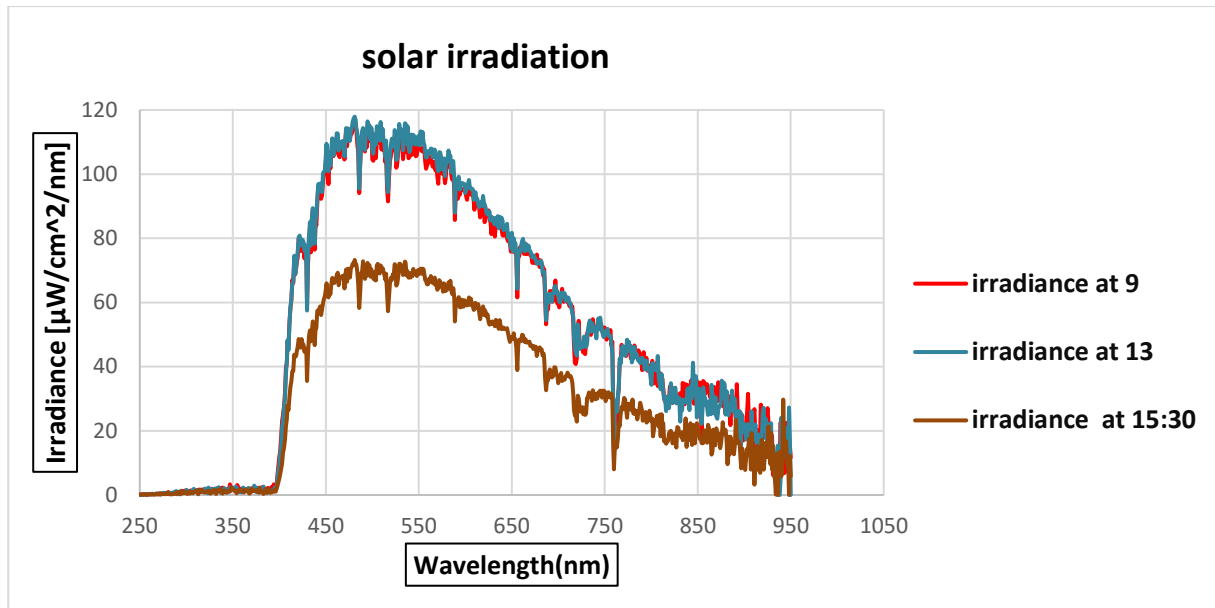
Figure 3.3. Irradiance-Segment D

3.3. Illuminance Measurement

Illuminance was measured with Konica Minolta CL-200A, this advanced lux meter will quickly show on the LCD screen the illumination and average values of measurements. Illuminance values can be easily compared and shown either in a percentage or a difference value. Our measurement was made at three different times and four car orientations on the 14 different surfaces. The four orientations of car were North-East, South-East, South-West, and North-West.
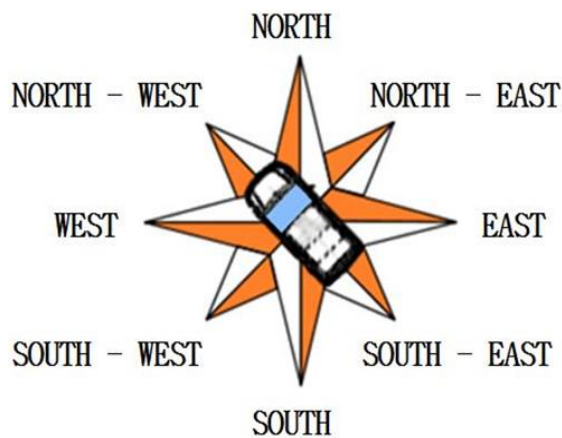
Figure 3.4. Cardinal direction of sample car

Figure 3.5. Interior surfaces of car

For calculating the luminous flux that every single surface at different segment received we tried to collect lux at three different times during the same day, and at each determined time we tried to put the car in the four different orientations, then computed an average based on the amount of lux received by each surface. Knowing the amount of Lux is important for analyzing the degradation of the interiors of vehicles, and also for stimulating the natural weathering in accelerated environment. In **table 3.1** the quantity of illuminance for "segment D" that was collected in a partly cloudy day on 5th June 2020 is listed. The amount of irradiance (w/m2) in the **table 3.1** were collected from "Atmospheric Physics Meteorological Station" website of Department of Physics, University of Turin. The data of illuminance for segment A and B has been listed in the appendix.

Table 3.1. Illuminance of segment D for 14 different surfaces

Time	Climate condition	Irradiance W/m2	Car orientation	Dashboard	Top left door	Top right door	Parcel shelf	Gear shift	Tunnel	Radio	Right seat	Left seat	DAB	Rear seat	Center right door	Center left door	Cluster
9:00	partly cloudy	600	SW	54600	44700	3760	56900	513	1860	26900	3990	2320	3420	51500	1923	1732	1728
9:00	partly cloudy	600	NW	46900	25500	39100	60700	2610	1860	2014	1366	879	2430	1663	1724	1262	1136
10:04	partly cloudy	826	NE	63100	4750	42900	56900	54600	3360	5410	2937	2315	2075	45800	1610	3250	1506
11:00	partly cloudy	578	SE	65400	43500	39100	52100	4980	5570	1964	4320	3190	2111	882	2791	2914	800
11:45	partly cloudy	501															
12:57	partly cloudy	428	SW	71500	49600	46100	74500	69400	3260	3250	48200	62000	6770	1336	3930	1820	1199
12:57	partly cloudy	428	NW	85700	65500	6470	81600	79500	1234	19350	2418	67500	29100	1190	1820	2148	1855
13:25	partly cloudy	925	NE	83200	52800	58000	81300	4400	1466	2004	2720	1184	1643	819	8090	8550	945
14:08	partly cloudy	862	SE	81500	4200	63400	77000	79300	2085	1180	68000	2157	27500	649	2066	1835	1132
15:18	partly cloudy	724	SW	59000	3930	45000	48700	56100	36800	2136	2920	43100	1862	683	1711	36400	1027
15:18	partly cloudy	724	NW	57200	44300	3850	46600	55500	53800	1442	44100	27600	1565	962	35500	1372	645
15:18	partly cloudy	724	NE	49100	39200	2735	55200	2813	1168	1297	749	1280	45600	1290	825	1675	29500
15:56	partly cloudy	642	SE	54300	3050	41300	56200	2820	1184	1793	1743	863	1052	573	1258	1187	491

Highest

Lowest

Table 3.2. Average illuminance between four different car orientation-Segment D

Time	Irradiance W/m2	Dashboard	Top left door	Top right door	Parcel shelf	Gear shift	Tunnel	Radio	Right seat	Left seat	DAB	Rear seat	Center right door	Center left door	Cluster
09:00	600	57500	29613	31215	56650	15676	3163	9072	3153	2176	2509	24961	2012	2290	1293
13:00	428	80475	43025	43493	78600	58150	2011	6446	30335	33210	16253	999	3977	3588	1283
15:30	724	54900	22620	23221	51675	29308	23238	1667	12378	18211	12520	877	9824	10159	7916

As it can be seen in **table 3.2,** for "segment D", dashboard, parcel shelf and gear shift have higher average daylight illuminance and center left door, center right door and cluster have lower average daylight illuminance.

Table 3.3. Average illuminance between four different car orientation-Segment A

Irradiance W/m2	Time	Dashboard	DAB	Radio	Cluster	Gear shift	Tunnel	Left seat	Right seat	Center left door	Top left door	Center right door	top right door	Rear seat	Parcel shelf
630	9:30	45598	9541	14240	2378	13744	2098	4107	19044	1346	38144	5421	27848	19491	23191
870	12:30	74600	8826	18338	2477	26688	25388	10053	5155	1285	34651	2074	34290	1599	33552
630	15:30	52020	3504	7243	1888	16676	13597	19397	13806	4168	38797	7174	40963	1409	23884

For "segment A", as it can be seen in **table 3.3** dashboard, top of the doors and parcel shelf has higher average daylight illuminance and center of the doors and cluster has lower average daylight illuminance.

Table 3.4. Average illuminance between four different car orientation-Segment B

Time	Irradiance W/m2	Dashboard	Top left door	Top right door	Parcel shelf	Gear shift	Tunnel	Radio	Right seat	Left seat	DAB	Rear seat	Center right door	Center left door	Cluster
09:00	690	50800	23330	16729	7573	27156	11383	4827	12710	8104	2092	14248	7764	2070	4571
13:00	982	72773	45593	44018	1444	4538	2176	1983	19065	28835	2172	886	4196	2196	1726
15:30	702	60575	35603	24704	6654	27044	14199	1826	11950	12774	10881	677	11377	11630	1126

For "segment B" dashboard and top of the doors has higher average daylight illuminance and DAB radio and cluster has lower average daylight illuminance.

Regarding to previous table the different interior parts of car received different illuminance during the day or even the same surface in the different orientation took diverse amount. In **figure 3.6**, I tried to show the quantity of Lux for segment D by different colors.
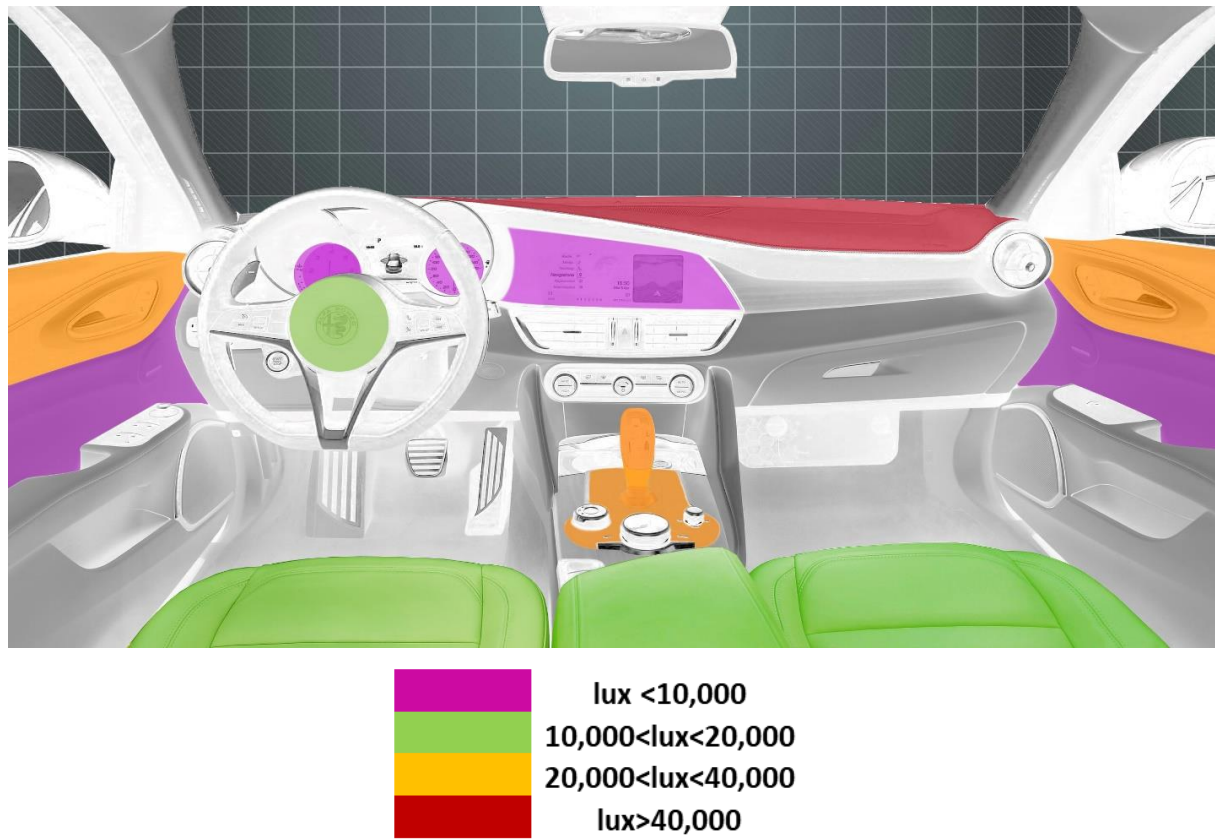
Figure 3.6. Demonstration of interior illuminance of segment D by colors

Table 3.5. Average daylight illuminance weighted to irradiance (lux)-Segment D

Surface	Exposition (Lux)	Ratio respect dashboard (%)
Dashboard	62038	100
Parcel shelf	59956	97
Gear shift	31685	51
Top right door	30911	50
Top left door	29999	48
Left seat	16384	26
Right seat	13605	22
Tunnel	11177	18
DAB	10003	16
Rear seat	9155	15
Center left door	5859	9
Center right door	5720	9
Radio	5370	9
Cluster	4027	6
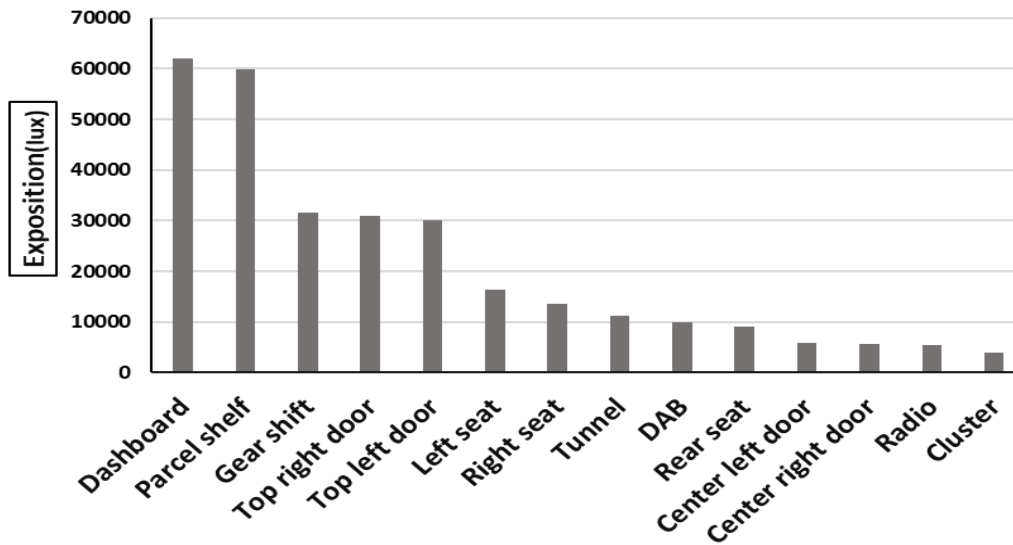
Figure 3.7. Average daylight illuminance weighted to irradiance (lux)-Segment D
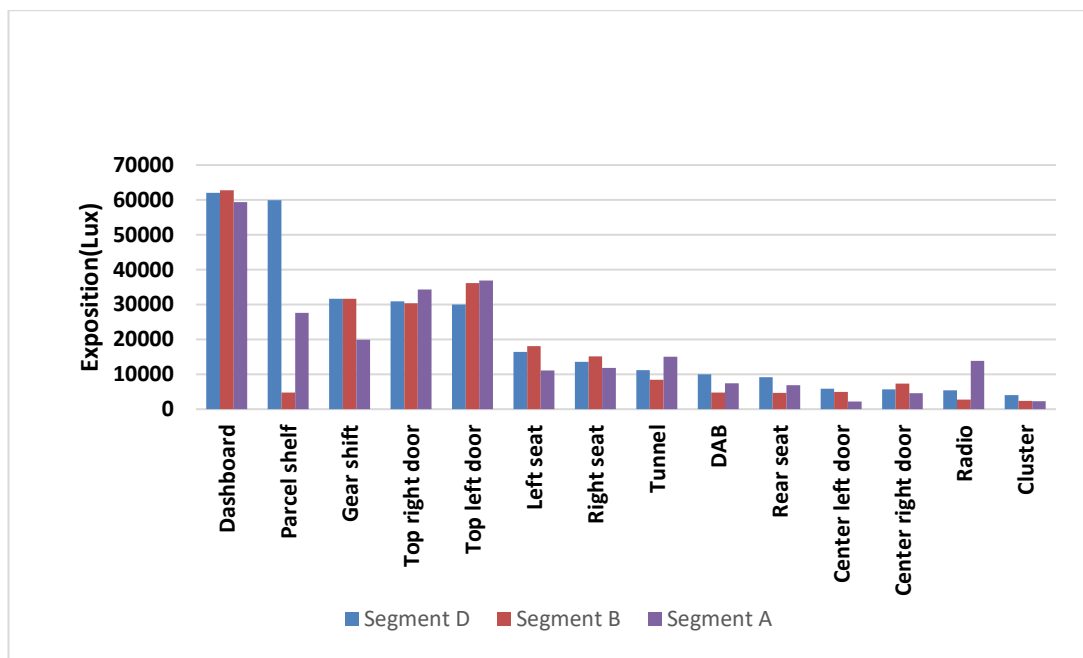
Figure 3.8. Comparison of Average daylight illuminance weighted to irradiance for 3 segments

With comparison of average daylight illuminance weighted to irradiance among 3 cars:

- Segment D received more than segment A in most of the surfaces except top of the doors, tunnel and radio

- Segment D received more than Segment B in different surfaces except right seat, left seat, top left door and center right door, and they received almost the same exposure in dashboard and Gear shift

- The ratio between the lowest (cluster) and the highest illuminance value (horizontal dashboard) in segment D is 6% and in the segment A and B is 4%.

3.4. Optical and Physical Characterization

3.4.1. Transparent Samples

During this survey one of the main goals was analyzing the optical characterization of our samples after natural and artificial weathering. Most of the samples that I examined after the weathering, the substrate was either polycarbonate or polycarbonate/poly methyl methacrylate in the form of transparent or black one with the high gloss finishing or matt finishing. These optical surfaces are mostly used in the cluster and infotainment sector.

3.4.1.1. Color Measurement

In **table 3.6**, different optical transparent surfaces are listed with the details of finishing that were subjected to the accelerated weathering in accordance with SAE J2412 standard. It will be interesting to see how the color and haze of transparent samples change when subjected to the specified exposures of 600kj, 900kj, and 1240kj in comparison to the reference sample with no exposure.

Figure 3.9 shows a significant increase of delta E in sample A and B which is not acceptable. we need more parameter for analyzing the behavior of those samples. As defined in the standard, the changes of color (ΔE) less than 3 is the suitable outcome, therefore for sample D, E and G the rate of increasing is suitable. Moreover, for sample H and I the rate of changes is less than 3.

Table 3.6. Color measurement of transparent samples

Surface	Substrate	Optical finishing	Delta E		
			600 KJ	900 KJ	1240 KJ
Sample A	PC	Matt	1.52	11.5	8.35
Sample B	PC	Matt	1.51	10.98	8.78
Sample D	PC	Matt	2.53	2.36	3.67
Sample E	PC	Gloss	2.24	2.74	3.2
Sample G	PC	Matt	1.39	2.18	4.41
Sample H	PC/PMMA laminated	Gloss	1.17	1	0.68
Sample I	PC/PMMA laminated	Gloss	1.1	0.99	0.61
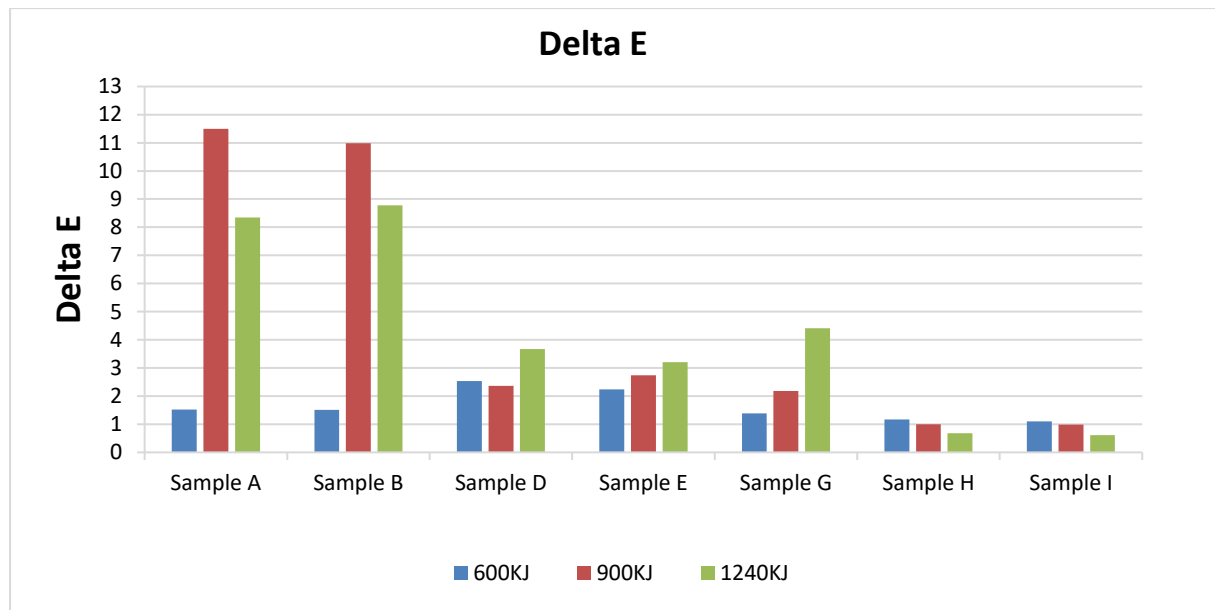
Figure 3.9. Delta E of transparent sample at different irradiation

3.4.1.2. Haze Measurement

Haze is another important optical parameter for studying our transparent samples after weathering, which will show us the amount of scattered light respect to incident light. As we predicted, all samples showed the output of the uptrend. As you can see, the haze of samples A and B below 900kj and 1240kj has a major change from the reference.

Table 3.7. Haze of transparent samples

Surface	Haze			
	Reference	600 KJ	900 KJ	1240 KJ
Sample A	0.66	0.98	6.03	10.51
Sample B	0.53	1.90	7.69	8.32
Sample D	0.43	0.58	1.19	1.07
Sample E	0.57	0.79	1.19	1.41
Sample G	0.59	0.59	1.40	4.22
Sample H	0.38	0.55	2.00	4.54
Sample I	0.32	0.59	2.17	6.17
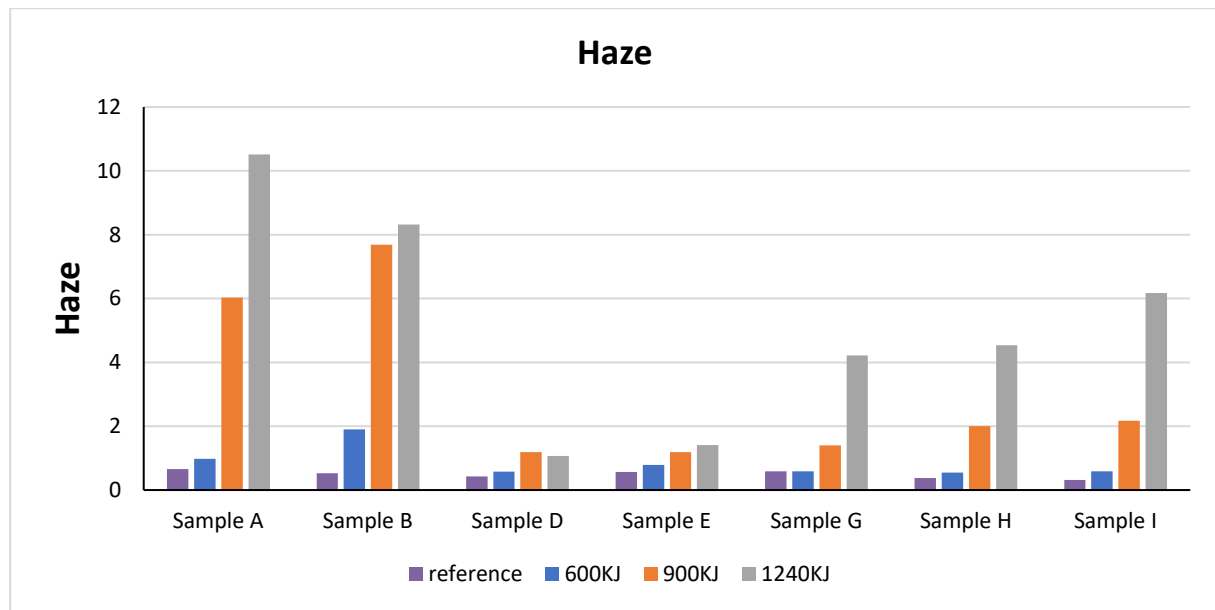
Figure 3.10. Haze of transparent sample at different irradiation
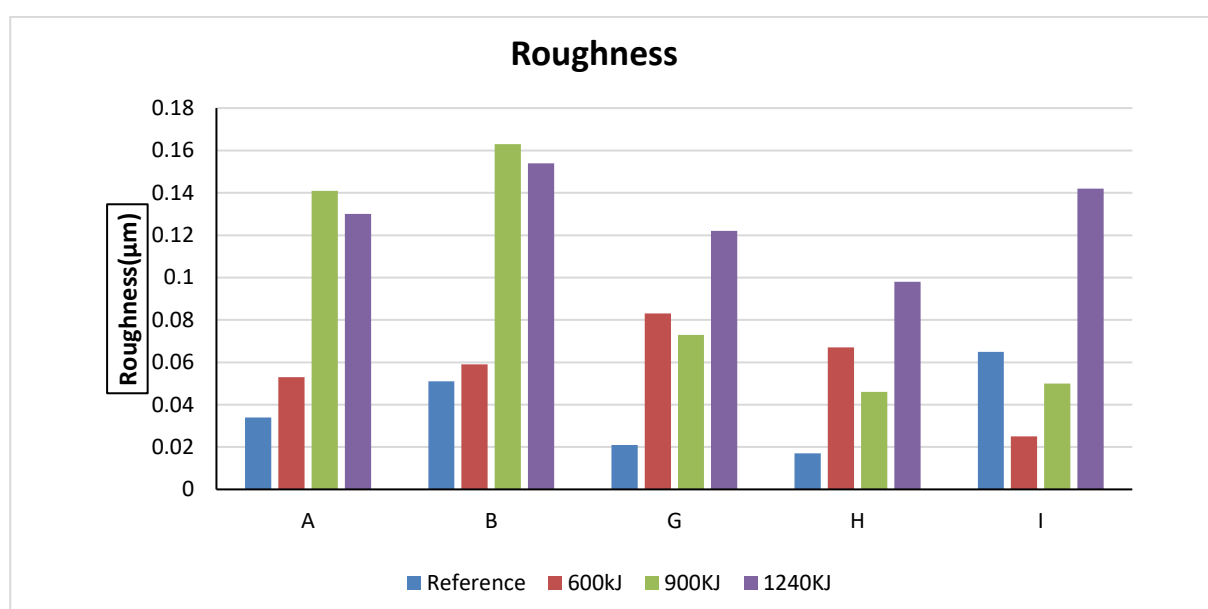
3.4.1.3. Roughness

Figure 3.11 has been demonstrated the roughness of my transparent samples which was made by profilometer Veeco Dektak150. In the case of sample, A and B the amount of roughness at reference and after weathering at 600kj is mostly equal. This means that the surface of our samples during accelerated weathering up to 600kj undergoes no significant changes. This small change in roughness before and after weathering could be confirmed by the appearance of the samples, which means that even the eyes cannot see the damage on the surface. However, with higher doses of irradiance at 900 kj and 1240 kj, roughness increases.

In the case of samples G and H, the same trend can be seen for both of them. The increase in roughness is obvious after 600 kj of exposure to the surface of the sample, but the next steep at 900 kj shows a slight decrease in roughness, which is not a significant amount. It can be stated that after 600 kj and 900 kj the roughness is more or less the same. It essentially means the same actions at 600kj and at 900kj. At last, under the 1240 kj exposure the amount of roughness is more than others.

For sample I, the strange result was being obtained for the roughness of the reference. It was higher than 600kj and 900kj, although all the measurements are in the micrometer unit and, in general, the difference between the reference and 600kj and 900kj is not that large but we didn't expect that. In the last step at 1240 kj, the roughness is greater than the previous one.

Table 3.8. Roughness of transparent sample at different irradiation

Surface	Roughness (µm)			
	Reference	600 KJ	900 KJ	1240 KJ
Sample A	0.034	0.053	0.141	0.13
Sample B	0.051	0.059	0.163	0.154
Sample D	0.021	0.083	0.073	0.122
Sample E	0.017	0.067	0.046	0.098
Sample G	0.065	0.025	0.05	0.142
Sample H	0.034	0.053	0.141	0.13
Sample I	0.051	0.059	0.163	0.154

Figure 3.11. Roughness of transparent samples at different radiation

3.4.2. Black Samples

A modern car is a large assemblage of parts made of various of materials. Many of these parts have a protective coating applied to improve the appearance or provide additional durability of the substrate. In many coating systems, the uppermost layer is a clear coating (5–50 µm in thickness), It not only protects the underlying layers or substrate from chemical and UV degradation, but it also protects against mechanical damage that can result in surface scratches. Consumers want a permanent, scratch-free finish on all parts of their vehicles, indicating that scratch performance is becoming the most important customer concern for automotive paint systems [83].

3.4.2.1. Color measurement

We analysed the color measurement and the haze of our transparent samples, which can be used in cluster and display. In other interior parts of the car, such as gear shifts, dashboard,

Chapter 3: Results and Discussion

DAB and doors, we can't use transparent ones, so we're going to paint a black on substrate. In this condition, it is better to measure the Gloss of our sample in order to understand how the surface of the samples is aged after weathering. In all cases, the measurement was averaged for 5 replicates of the specimen.

Table 3.9. Gloss of black samples

Surface	Substrate	Optical finishing	Roughness (µm)			
			Reference	600 KJ	900 KJ	1240 KJ
Sample A	PC	Matt	85.7	86.1	82.5	72.9
Sample B	PC	Matt	85.4	84	84.6	67.6
Sample D	PC	Matt	79.7	69.78	49.5	-
Sample E	PC	Gloss	80.2	72.08	59.74	-
Sample G	PC	Matt	85.7	81.8	45.8	44.1
Sample H	PC/PMMA laminated	Gloss	84.7	87.9	85.6	79.8
Sample I	PC/PMMA laminated	Gloss	86.8	87.8	85.4	82.9
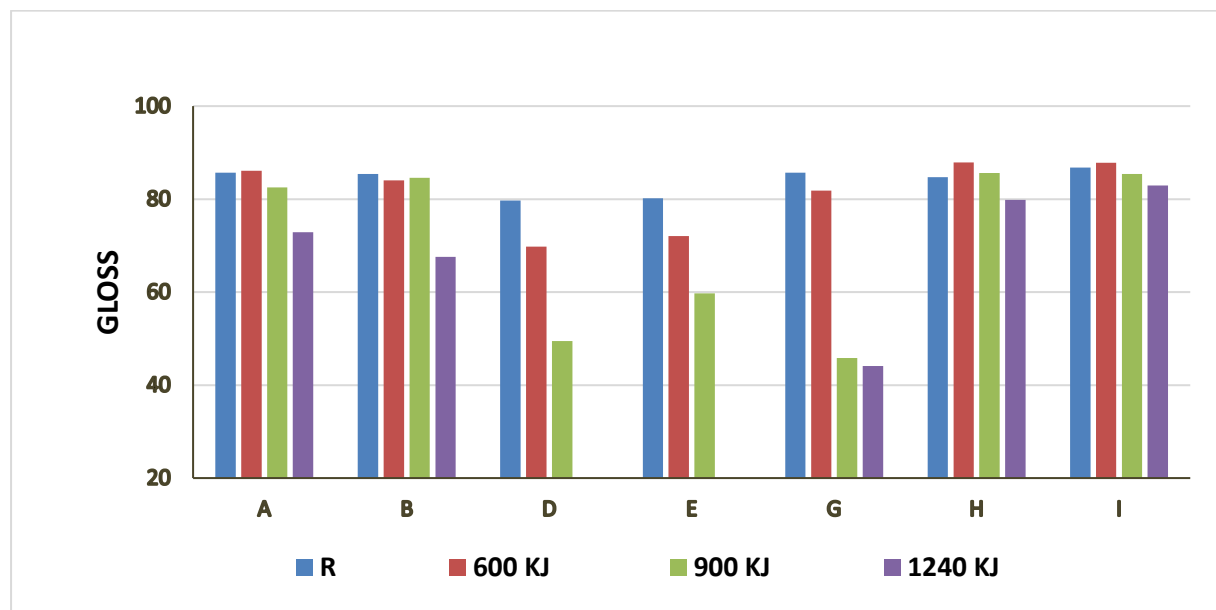
Figure 3.12. Gloss of black samples at different radiation

For better understanding the deviation of gloss, I am going to show the variation respect to the reference sample. Unfortunately, I did not measure gloss for samples D and E at 1240 kj because they were damaged. If the variation is less than 20%, we can state that this amount of variation is acceptable. As performed in the following table, the changes of Gloss for sample A, B and H and I is suitable, but for sample D, E and G under 900kj and probably at 1240kj is bigger than 20%.

**Table 3.10.** Variation of gloss of black samples

Surface	ΔGU/GUTQ (%)		
	600 KJ	900 KJ	1240 KJ
Sample A	0.47	3.76	15
Sample B	1.64	0.91	20.79
Sample D	12.4	37.9	!
Sample E	10.1	25.5	!
Sample G	4.5	46.5	48.5
Sample H	3.71	1.02	5.83
Sample I	1.08	1.68	1.56

3.4.2.2. Roughness

In this section, we investigate to know the correlation of roughness of our samples with all optical parameters like color measurement and gloss, far along in particular, the relationship between roughness and all field parameters (Sa, Sq, Ssk, Sku), more over with these areal field parameters we will see how the topographic of our sample has changed. Because of this important issue, we have tried to measure the roughness of the surface three times and then make the average.

After analysing our data and reviewing our topographic images, which were extracted by a confocal microscope (Leica DCM8), I decided to measure again for samples A and B, and finally, we achieved the brilliant and expected results due to weathering by using a microroughness filter. When microroughness filtering is used, this operator is employed to cancel the noise, and then it is used to extract the real roughness value.

The raw data in the **Figure 3.13**, before using a microroughness filter, and in the **Figure 3.14** the result after applying the filter has been demonstrated. As you can find in the first graph the difference of roughness after exposure and reference in some of them is not well. But after that when microroughness filter was used, the result for sample D, E, G, H, I, has been increased due to weathering. Just for sample A and B at the reference the roughness was higher than 600kj.
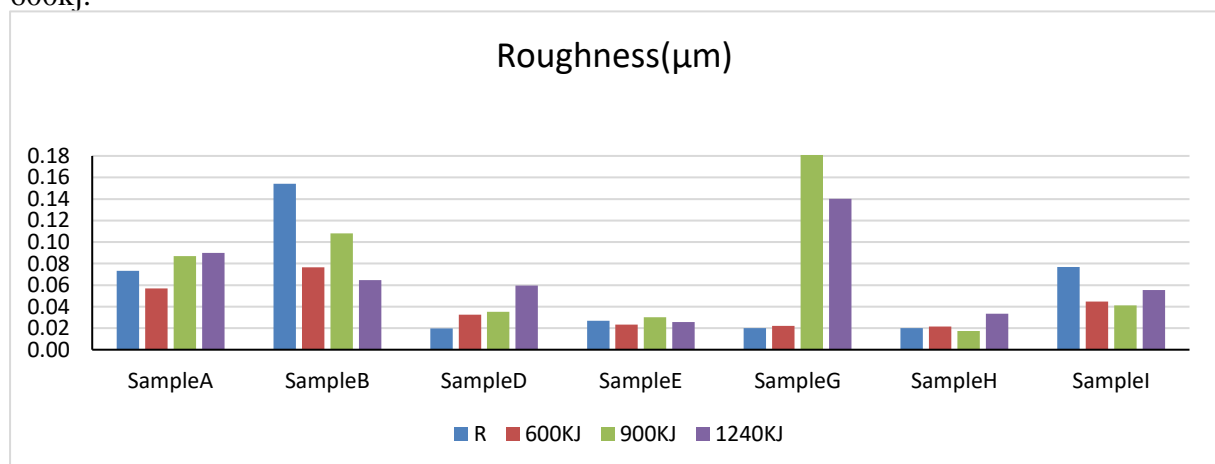
Figure 3.13. Roughness of black sample (without using filter)

Chapter 3: Results and Discussion

Table 3.11. Roughness of black samples (without using filter)

Surface	Roughness (µm)			
	Reference	600 KJ	900 KJ	1240 KJ
Sample A	0.0733	0.0569	0.0870	0.0898
Sample B	0.1540	0.0765	0.1080	0.0646
Sample D	0.0196	0.0327	0.0351	0.0596
Sample E	0.0270	0.0234	0.0303	0.0256
Sample G	0.0200	0.0221	0.2239	0.1403
Sample H	0.0199	0.0215	0.0175	0.0335
Sample I	0.0769	0.0448	0.0413	0.0555
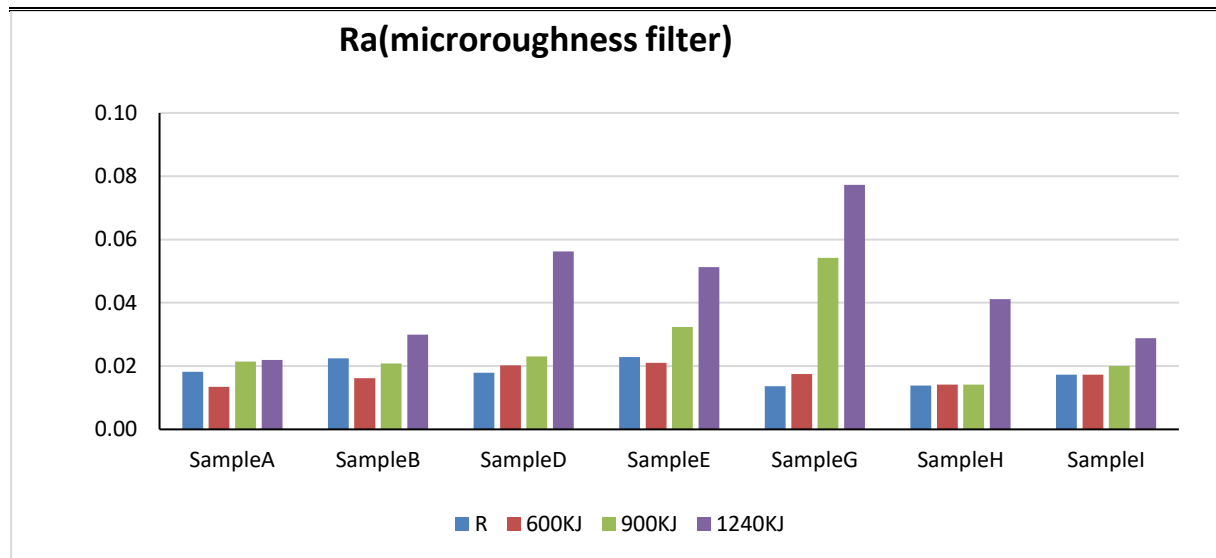
Figure 3.14. Roughness of black samples with using microroughness filter

Table 3.12. Roughness of black samples with using microroughness filter

Surface	Roughness (µm)			
	Reference	600 KJ	900 KJ	1240 KJ
Sample A	0.0182	0.0134	0.0214	0.0219
Sample B	0.0224	0.0162	0.0208	0.0299
Sample D	0.0179	0.0202	0.0231	0.0562
Sample E	0.0228	0.0210	0.0324	0.0513
Sample G	0.0136	0.0175	0.0542	0.0773
Sample H	0.0138	0.0141	0.0142	0.0412
Sample I	0.0173	0.0173	0.0200	0.0288

3.4.2.3. Areal field parameter

Skewness

For the characterization of the surface height, and in particular the shape of the topography of the height distribution, the skewness was chosen. For black samples, A and D have the same substrate, as well as B, E and G the polycarbonate substrate. The only difference is the coating, which relates to the different supplier. The substrate of sample H and I was the same, PC/PMMMA but provided by different supplier.

When visualizing an amplitude distribution curve, skewness represents the degree of bias in the vertical or horizontal direction. If you have a symmetrical profile, your amplitude distribution curve will be symmetrical about the center line. In contrast, an unsymmetrical profile will yield a skewed curve. If the bulk of the material is above the mean line, the skew will be negative; if the bulk of the material is below the mean line, the skew will be positive (positive skew). A concrete example, a porous, sintered or cast-iron surface will have a large skewness value. A good bearing surface has a negative skew, as this indicates the presence of comparatively few peaks that wear away quickly, as well as comparatively deep valleys to retain lubricant traces. Having a positive skew, it is likely that a surface will have poor lubricant retention, as there are no deep valleys to retain lubricant traces. Positively skewed surfaces, such as rounded or warped surfaces, have highly peaked features that project above the mean line. As I expected, the sample A and D have the same behavior and sample B, E and G have the similar trend. Also sample H and I have similar performance.
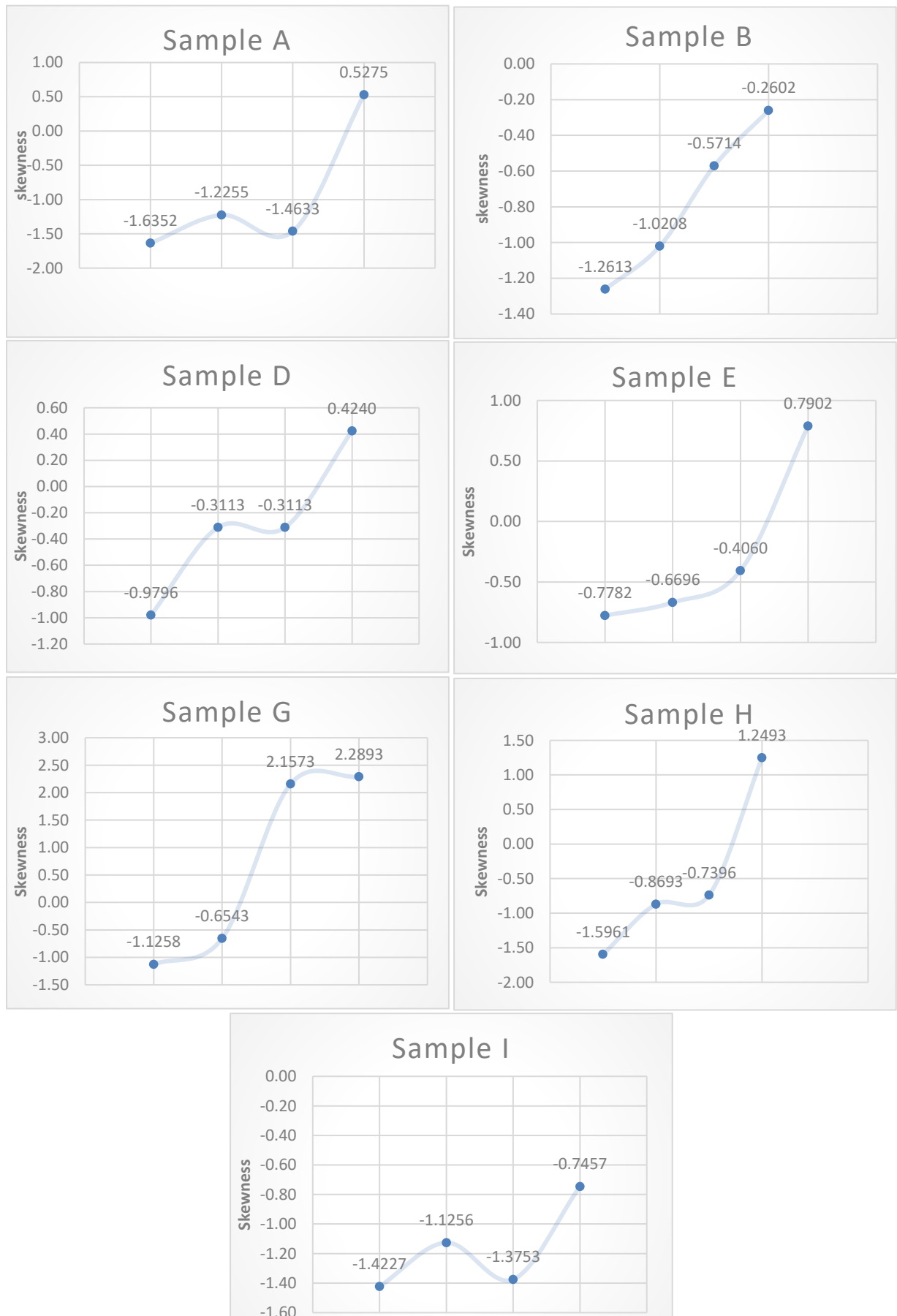
Figure 3.15. Skewness of black samples

Kurtosis

The Sku parameter is a measure of the sharpness of the surface height distribution, unlike Ssk, use of this parameter not only detects whether the profile spikes are evenly distributed but also provides a measure of the spikiness of the area. A spiky surface has a high kurtosis value, whereas a bumpy surface has a low kurtosis value. A surface with a Gaussian height distribution has a kurtosis value of three. For having a better idea about the height parameter, I plotted all values on one **Figure 3.17** for each sample. It can be seen that the Kurtosis of sample A and D have same trend, but not for the other samples.
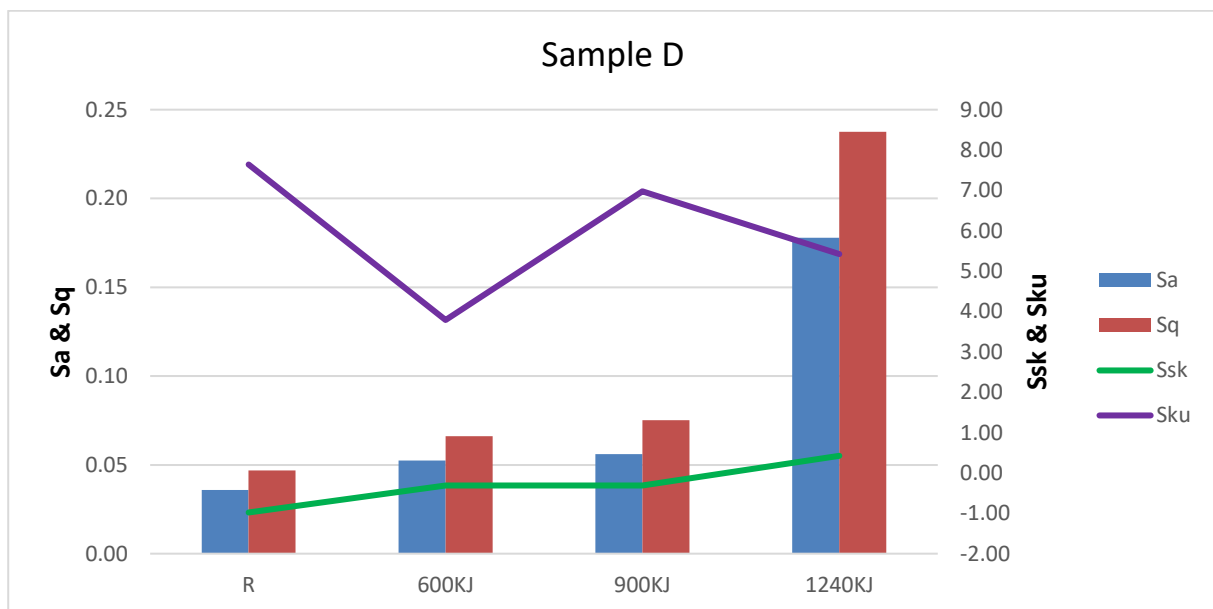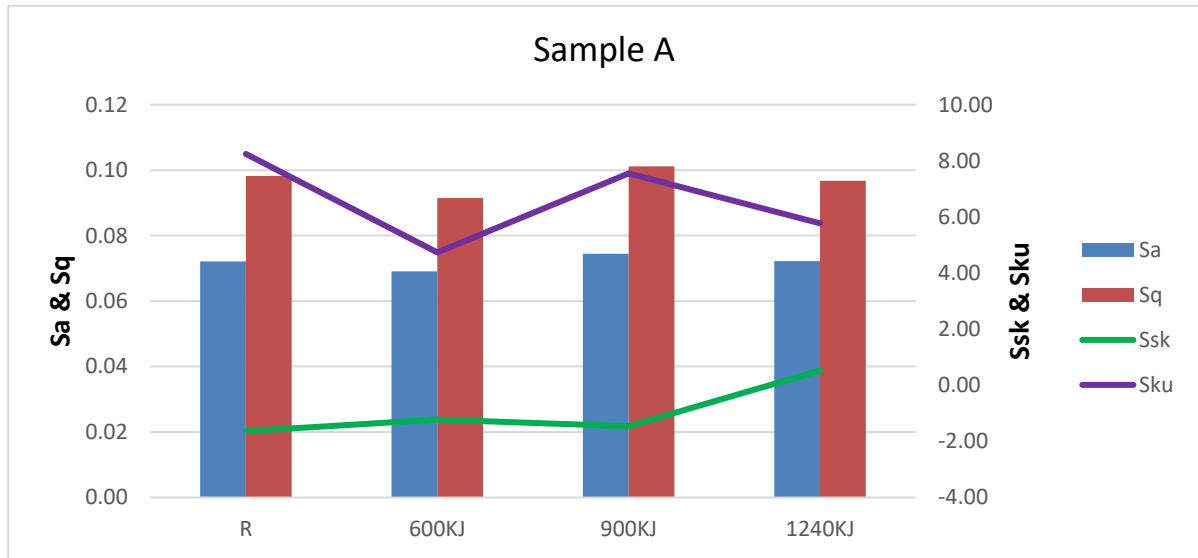
Sample B
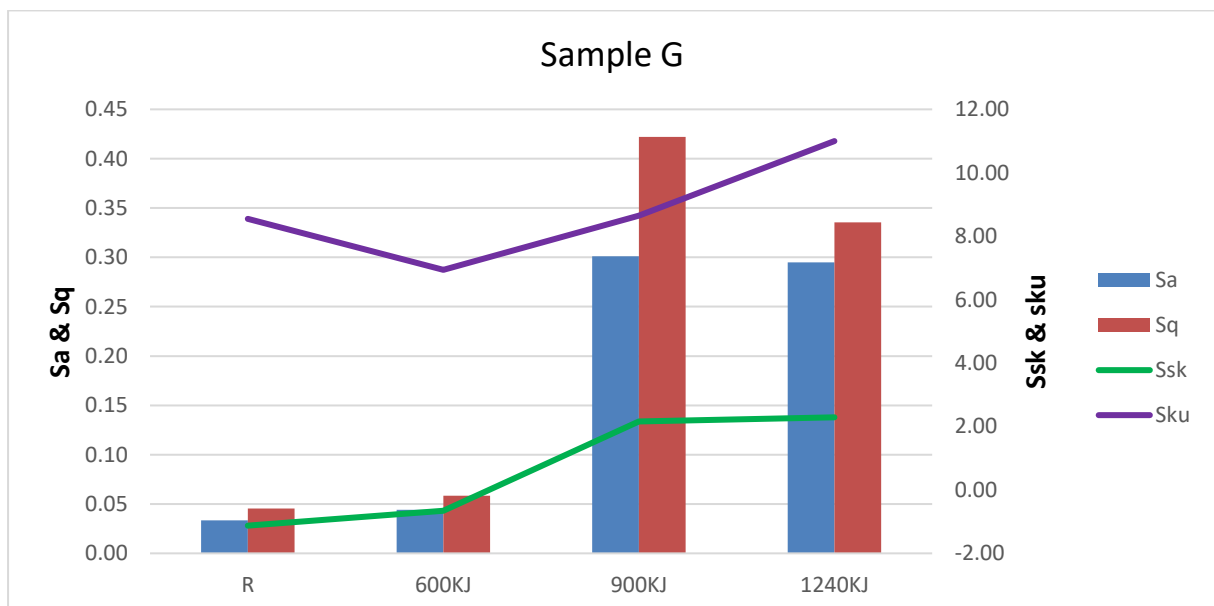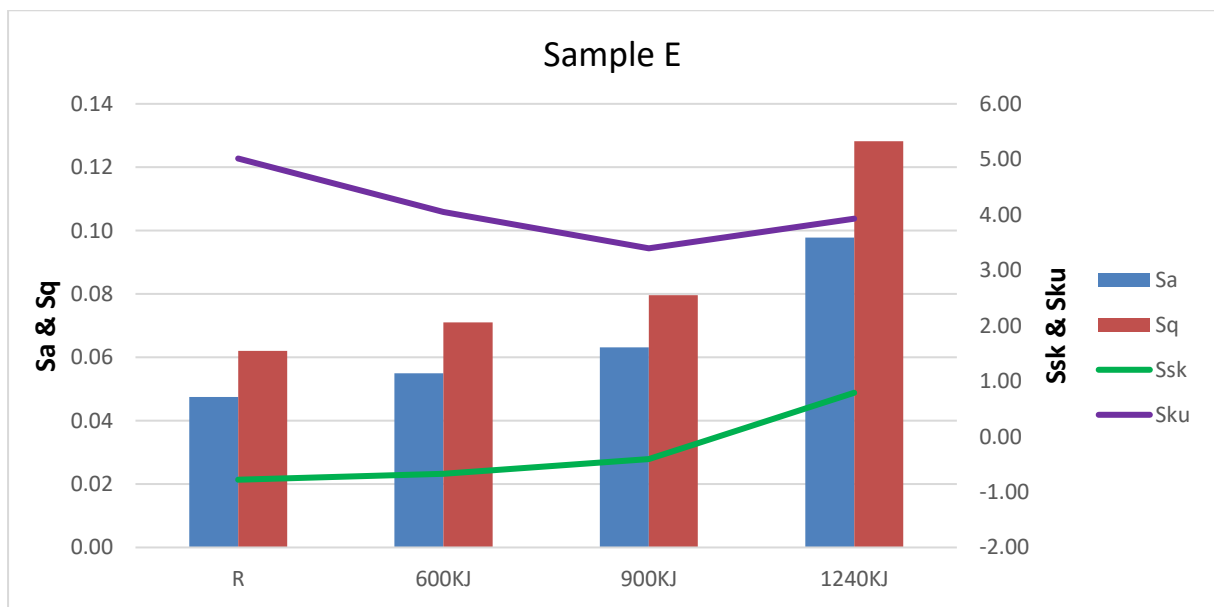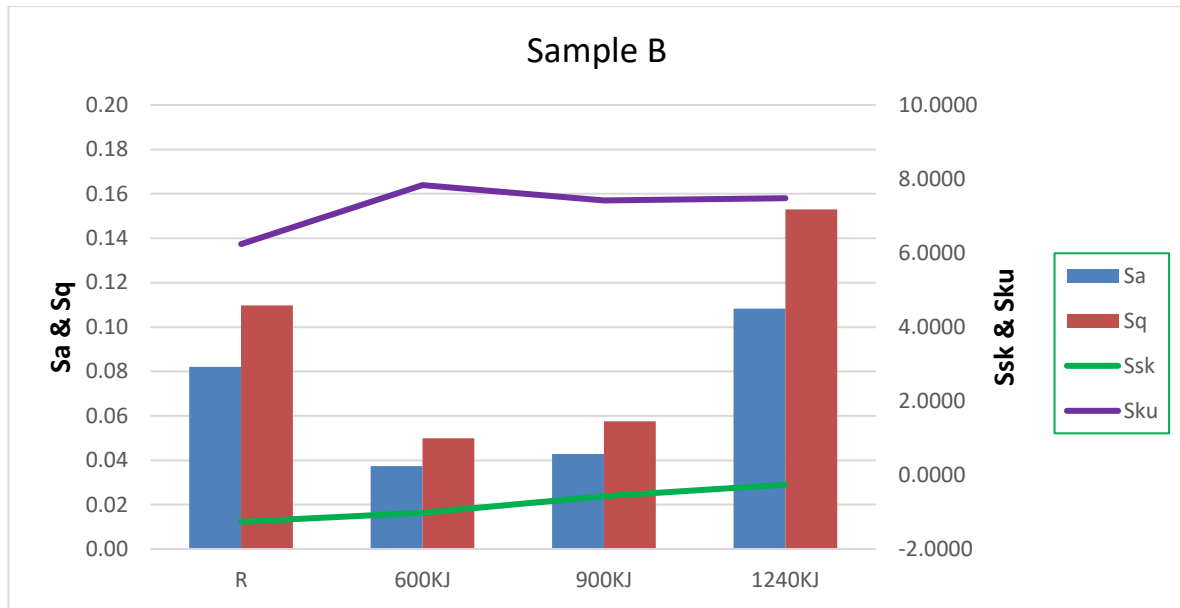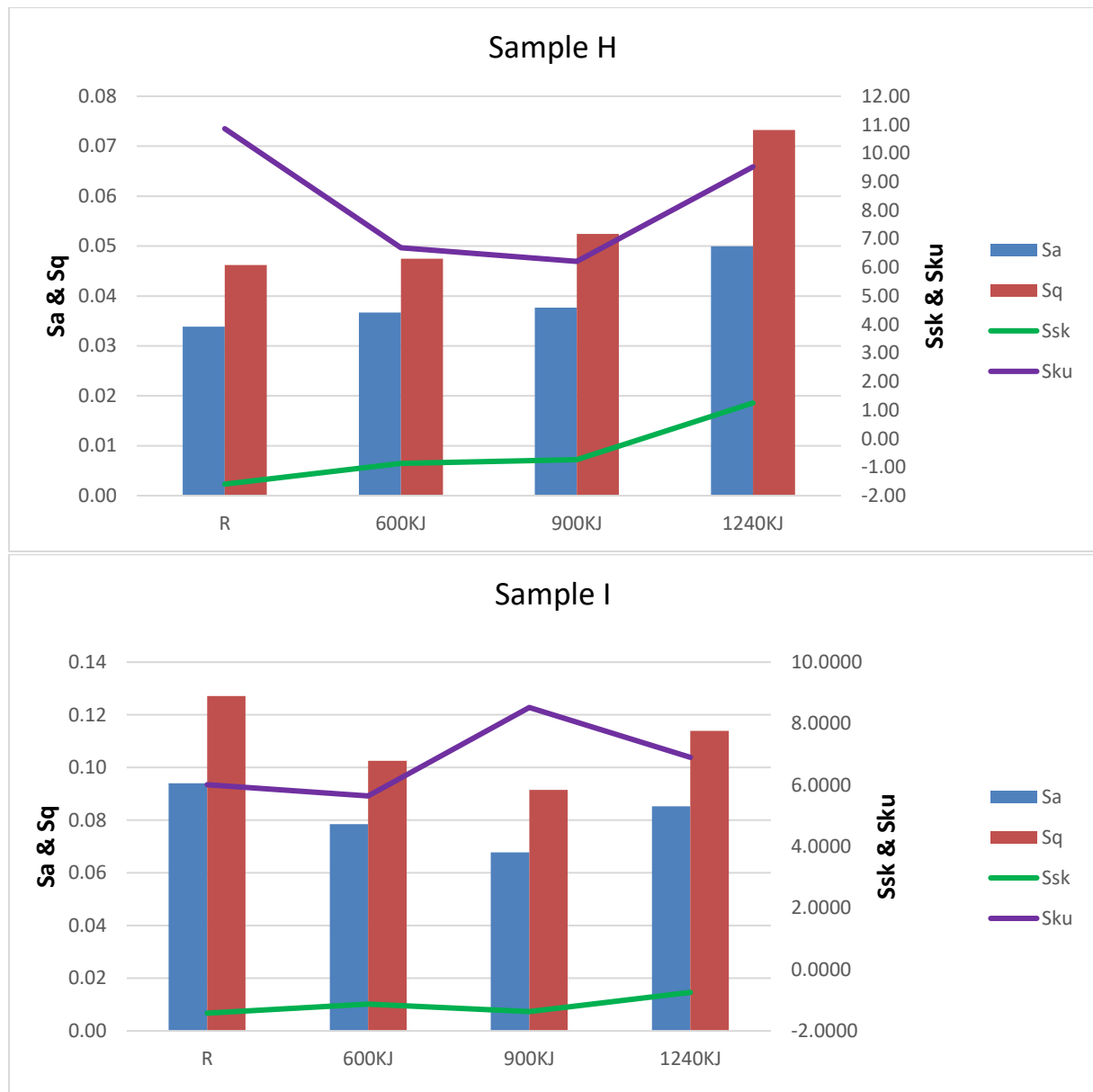
Sample E

Sample G

Figure 3.16. Kurtosis of black samples

Mean Height of the surface and Gloss

The relationship between root mean square height (Sq) and arithmetic mean height (Sa) with gloss has been demonstrated in this section. The relationship could be expressed with linear fit function $y = a + b*x$. The high correlation ($R^2 > 0.90$) for samples E, G, and B indicated that the gloss was highly dependent on surface roughness.

The relation between gloss and roughness is not as strong for samples D and H as it is for the previous ones, but it is still strong, and finally, the slightly relation for samples A and I. Later on, the correlation between variation of roughness (Ra) and variation of gloss (G) has been demonstrated.

Sample A

y = -275.76x + 108.53
R² = 0.0331

Sample A

y = -858.79x + 143.62
R² = 0.0952

Sample D

y = -979.05x + 127.79
R² = 0.8459

Sample D

y = -1213.7x + 124.76
R² = 0.7241

Sample B

y = -141.25x + 93.476
R² = 0.6361

Sample B

y = -252.91x + 95.089
R² = 0.9833

Sample E

y = -1163.8x + 153.21
R² = 0.9826

Sample E

y = -1311.9x + 143.1
R² = 0.9923
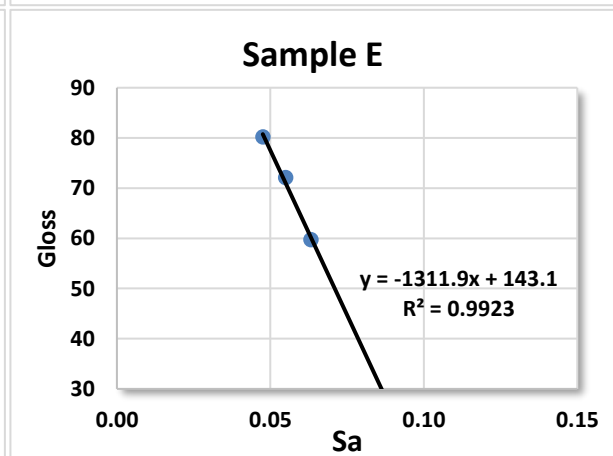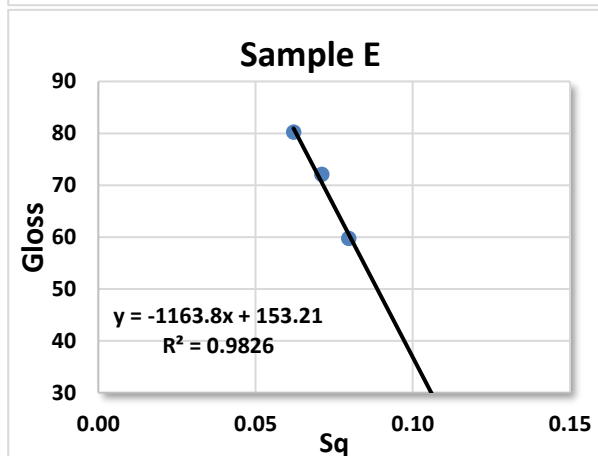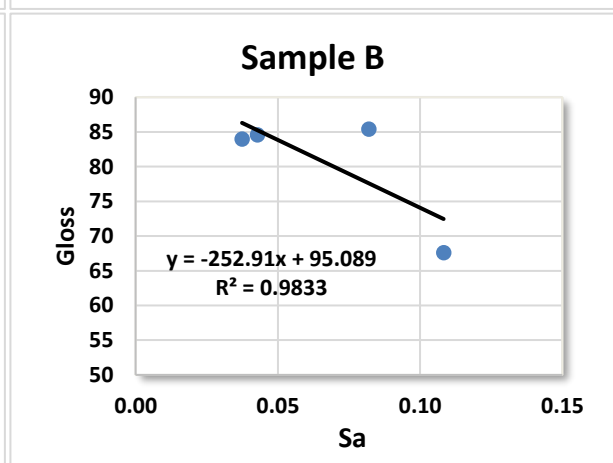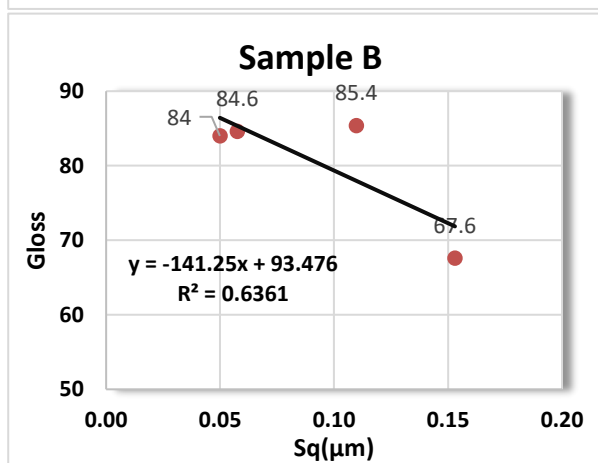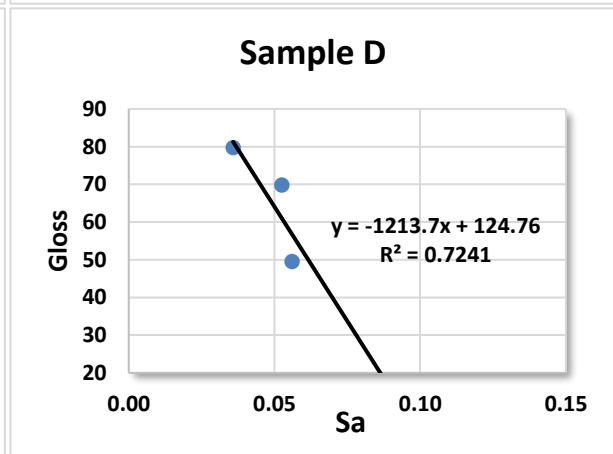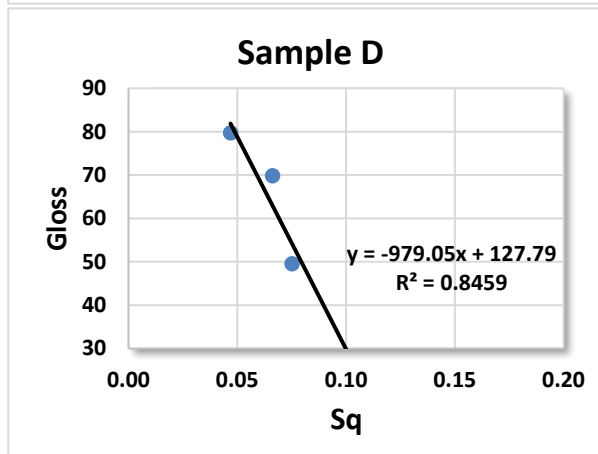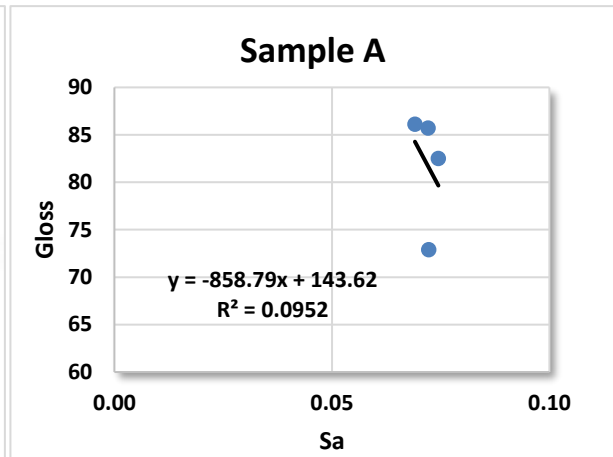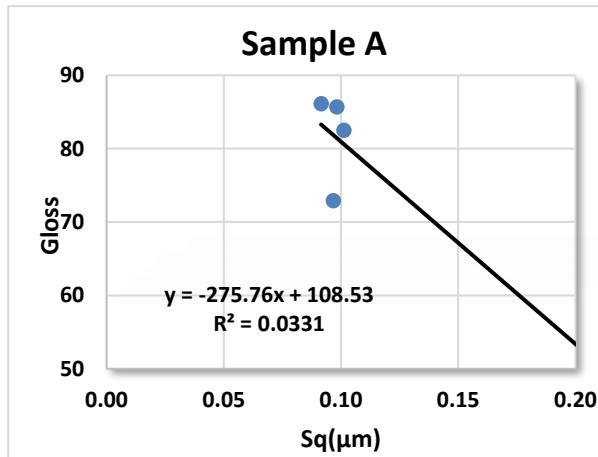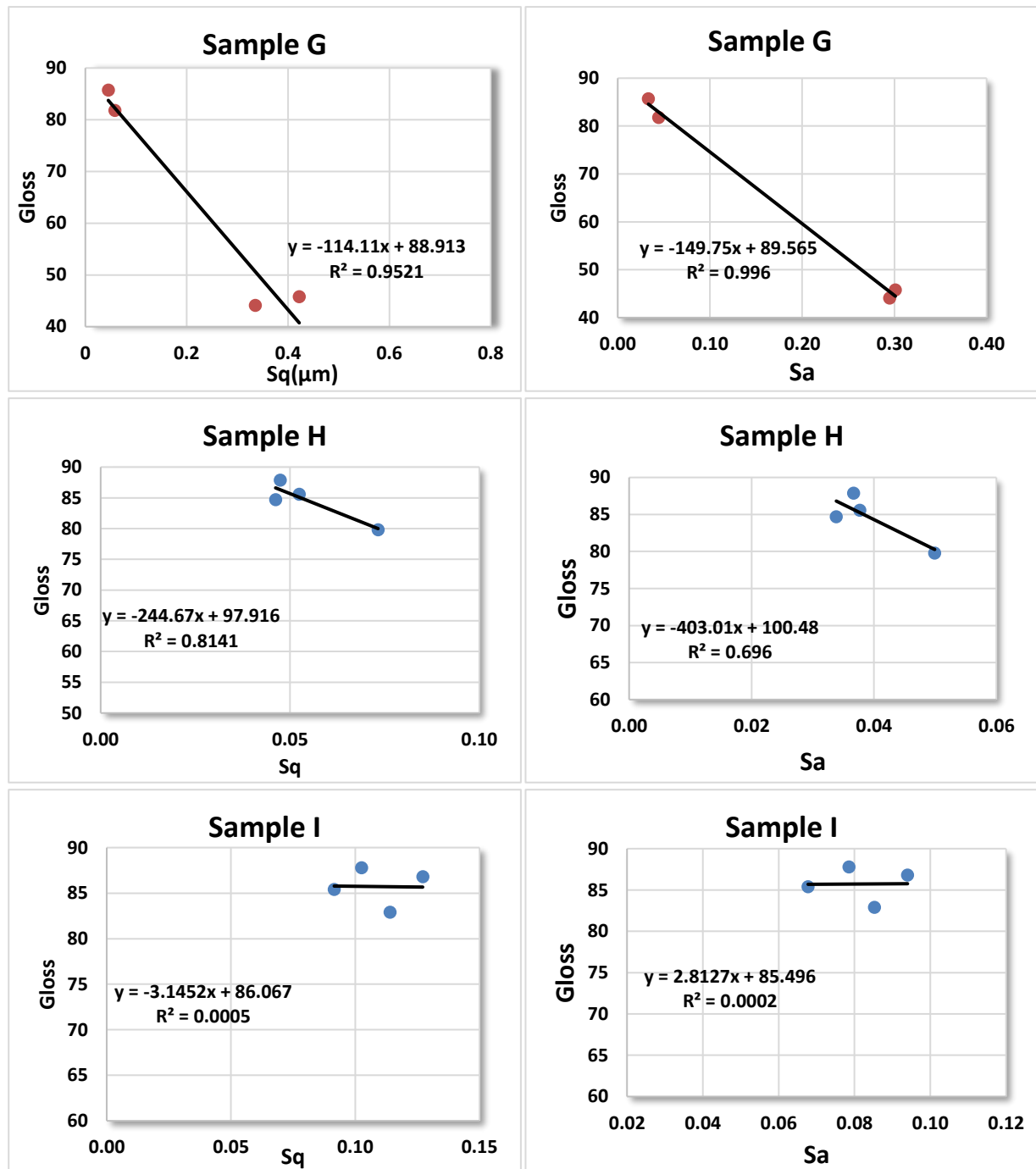
Figure 3.17. Correlation between Gloss and Sq- Sa for black samples

Samples	Correlation of Gloss with	
	Sq	Sa
A	0.63	0.98
B	0.98	0.99
D	0.95	0.99
E	0.033	0.095
G	0.84	0.72
H	0.81	0.69
I	0.005	0.002

3.4.3. Sample K and L

As previously stated, these two samples were used as display coverlens in "segment A" and "segment B". I attempted to measure roughness and gloss, and we also have color measurements from the Florida location. All of the samples that were analysed were stored in the Q-Lab environment in Florida for a period of 12 months for natural weathering. The total radiation dose received by these samples was approximately 5,174 MJ/m².

As previously mentioned, the substrate of sample K and L is PC with Anti-Glare finishing, however, in order to obtain a consistent result, the solution was applied to three different samples (K1, K2, K3…).

The gloss in CRF has been quantified five times for each sample in the black part. In the table below, you can compare my measurement to Q-lab's result. The result for sample3 is coherent but the result for sample4 is not, this could be due to the environmental factor such as temperature and humidity.

Furthermore, the adhesion test was performed on all samples; the coating on sample K was not removed, but it was removed from the sample L.

Table 3.13. Gloss of sample K and L

Surface	Adhesion	Gloss (12 months)	
		CRF	Florida
Sample K1	N.R	32.22	34
Sample K2	N.R	32.4	34
Sample K3	N.R	32.3	35
Sample L1	R	18.7	21
Sample L2	R	18.98	25
Sample L3	R	18.74	25

3.4.3.1. Color measurement

In this section, simply the results of Q lab testing have been analyzed, which were examined for Black part of display and transparent area separately. And hopefully, the variation of color after 12 months of weathering was acceptable for both of them.

Table 3.14. Color measurement of sample K and L

Black area	Delta E		
	6 months	9 months	12 months
TYPE K*	0.30	0.37	0.65
TYPE L*	0.35	0.82	1.06
Transparent area			
TYPE K**	0.43	0.78	1.51
TYPE L**	0.51	0.24	0.33
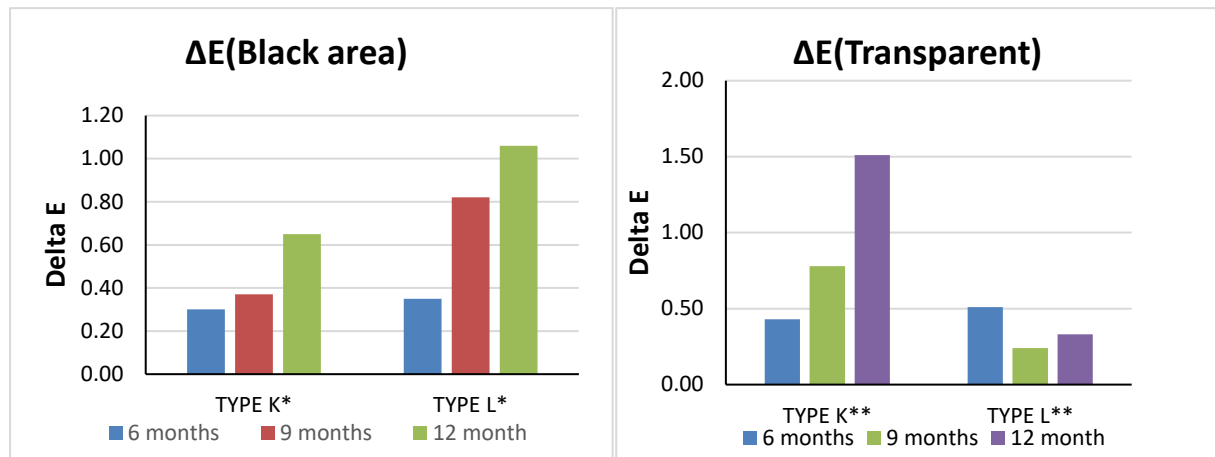
Figure 3.18. Color measurement at transparent and black area of sample K and L

3.4.3.2. Roughness

Stylus profilometer has been used to measure the roughness of samples K and L. To get a better idea of the effect of natural weathering after a year. Measurement of the black and transparent areas had been done separately, and then compare each part to the reference sample. As shown in the tables below, the changes in roughness after weathering were negligible.

Table 3.15. Roughness of sample K and L

Black area	Roughness (µm)				
	Reference	A	B	C	Average
Sample K	0.53027	0.49575	0.41176	0.503407	0.470306
Sample L	0.246113	0.278843	0.228973	0.22877	0.245529
Transparent area					
Sample K	0.469267	0.4371	0.458513	0.45568	0.450431
Sample L	0.217173	0.24997	0.237117	0.238037	0.241708

3.5. Conclusion

The data obtained from this study on the irradiance and illuminance of three segments revealed that the most important parts of the vehicle that must be made of high-quality polymers are the dashboard, parcel shelf, top of the doors, and gear shift.

The gloss, roughness, and color measurements of sample K and L after 12 months of natural weathering have been analyzed and confirmed. These samples are made of polycarbonate with antiglare finishing and are currently used in segments A and B.

The color, haze, and roughness variation of transparent samples was studied, and the results showed that the changes in parameter for sample D, E, G, H, I after radiation were suitable, but for sample A and B was acceptable under 600 kj but not more radiation. Since these polymers will be used in the future, they must be re-evaluated.

Chapter 3: Results and Discussion

For the black samples, the gloss variation of sample A, B, H, and I was less than 20%, which was within acceptable limits. However, for samples D, E, and G, the acceptable limit was 600kj, not more. By increasing the radiation, the roughness of all samples was slightly increased. As expected, increasing the roughness reduced the gloss of the samples.

Finally, when it comes to analyzing areal field parameters, the correlation of Sa and Sq with gloss shows that sample A and I have the smallest relation, while the other samples have a strong correlation. Sample A should be re-evaluated.

With studying height parameters specially skewness and kurtosis the graphs' tendency for similar substrate and coting was expected to be the same. This theory holds true for skewness; it can be seen, the same tendency for samples A and D. As well as the same skewness behavior for samples B, E, and G.

However, only sample A and D performed similarly on the kurtosis graph. The others need to be evaluated again.

To end, concerning the issue that sample M, N and P will be used in future, roughness and gloss were measured. For sample M, which was polycarbonate with high gloss finishing, the roughness has been increased slightly by increasing the radiation and due to that the gloss has been decreased. Sample N, which was polycarbonate with anti-glare finishing, did not change in roughness but increased in gloss when subjected to 600kj, 900kj, and 1240 kj. Sample P with matt finishing needs to be measured again at the reference because the roughness, which is mostly the same under radiations, is less than the reference, which is not reasonable and the gloss of sample P has been increased.

Appendix

Figure A.1. Demonstration of interior illuminance of segment A by colors

Table A.1. Illuminance of segment A for 14 different surfaces

Segment A				Dashboard	DAB	Radio	Cluster	Gear shift	Tunnel	Left seat	Right seat	Left door - center	Top Left door	Right door - center	Top Right door	Rear seat	Parcel shelf
Time*	Climate condition	Irradiance W/m²	Car orientation	Illuminance (lux)													
9:00	Clear	600	SW	44770	28800	30000	3797	5580	1962	4840	3720	899	38825	3624	7126	39992	38000
9:15	Clear	625	SE	57390	4139	5301	1895	18730	2516	4976	32390	1104	41650	15900	50760	1798	3705
9:20	Clear	620	NE	50200	2323	15760	1931	26720	2956	4539	36750	2167	37320	1447	45860	34860	4439
9:25	Clear	633	NW	30030	2901	5899	1889	3946	958	2073	3316	1214	34780	714	7645	1313	46620
9:48	Clear	663															
12:15	Clear	870	SW	79500	13720	20460	2238	45130	35030	25590	5878	977	57340	3291	10690	1666	4842
12:20	Clear	870	SE	78520	15330	22780	2382	53000	63470	4262	7099	2732	9820	1637	63960	1400	3466
12:25	Clear	870	NE	69140	2034	16720	1500	3920	1562	2758	4417	511	7772	1725	54800	1051	64450
12:27	Clear	870	NW	71240	4219	13390	3786	4703	1490	7603	3226	921	63670	1642	7709	2278	61450
12:52	Clear	884															
14:57	Clear	754															
15:20	Clear		SW	62460	3809	7886	1800	30260	50330	38040	12390	13910	53320	1306	51930	1187	2984
15:24	Clear		SE	43400	1890	8506	1079	3335	1189	2169	3860	814	5886	1395	47530	1600	44540
15:28	Clear		NE	42840	2092	4327	2395	2530	843	3027	1963	590	45890	603	6130	770	44940
15:32	Clear		NW	59380	6223	8251	2277	30580	2025	34350	37010	1358	50090	25390	58260	2080	3070

Figure 0.2. Average daylight illuminance weighted to irradiance (lux)-Segment A

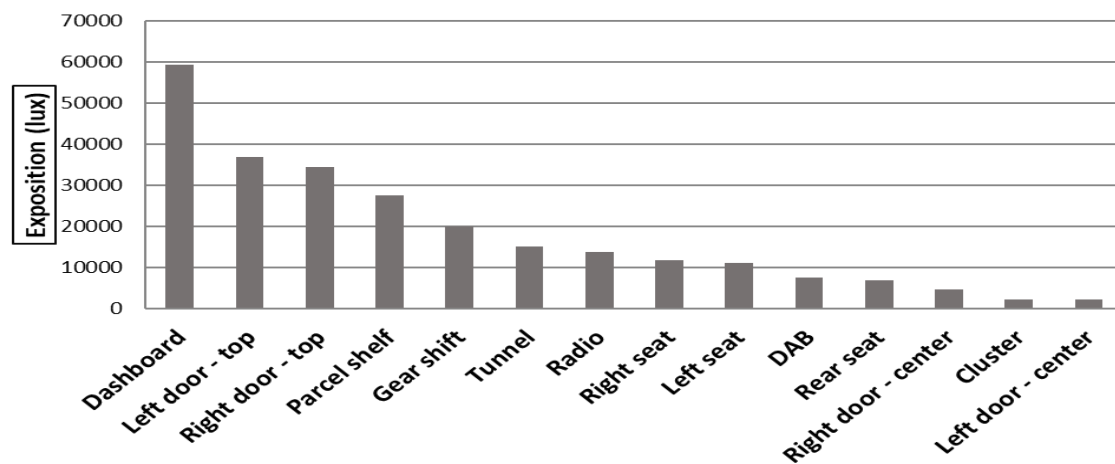| | lux <10,000 |
	10,000<lux<20,000
	20,000<lux<40,000
	lux>40,000

Figure A.3. Demonstration of interior illuminance of segment B by colors

Table A.2. Illuminance of segment B for 14 different surfaces

Segment B				Dashboard	Top left door	Top right door	Parcel shelf	Gear shift	Tunnel	Radio	Right seat	Left seat	DAB	Rear seat	Center right door	Center left door	Cluster
Time	Climate condition	Irradiance W/m2	Car orientation	Illuminance(lux)													
8:59	clear	603	SW	55900	44100	2400	1305	52200	802	1480	1100	27000	1489	28100	1035	4680	14660
8:59	clear	603	NW	32700	3830	1745	27400	1605	681	1328	820	1850	2430	345	820	820	1113
9:34	clear	690	NE	58900	3090	61600	845	3620	42200	13700	45700	1150	1600	28000	2300	780	1050
9:34	clear	690	SE	55700	42300	1169	740	51200	1848	2800	3220	2415	2850	546	26900	2000	1460
11:20	clear	905															
12:45	clear	1002	SW	87400	57200	48600	1182	4170	1959	1926	3040	42600	2349	1198	2473	1130	2126
13:17	clear	982	NW	91700	69500	10070	1631	4520	2245	2217	3170	66500	3280	887	1810	3950	2562
13:17	clear	982	NE	20290	47200	50800	1806	3040	1889	1680	3250	3750	1254	785	9220	1122	1105
13:33	clear	1036	SE	91700	8470	66600	1156	6420	2610	2107	66800	2490	1805	675	3280	2580	1112
15:39	clear	702	SW	63200	42300	49300	1225	58100	51000	1825	42200	2236	1623	624	1794	42300	1085
15:39	clear	702	NW	64100	51000	1336	1011	45800	2466	3370	2197	45900	1808	756	41400	1510	1397
15:39	clear	702	NE	57000	45500	3680	3280	1877	1876	855	1435	1743	38700	602	796	1876	1086
15:39	clear	702	SE	58000	3610	44500	21100	2400	1452	1252	1968	1215	1393	725	1518	833	936
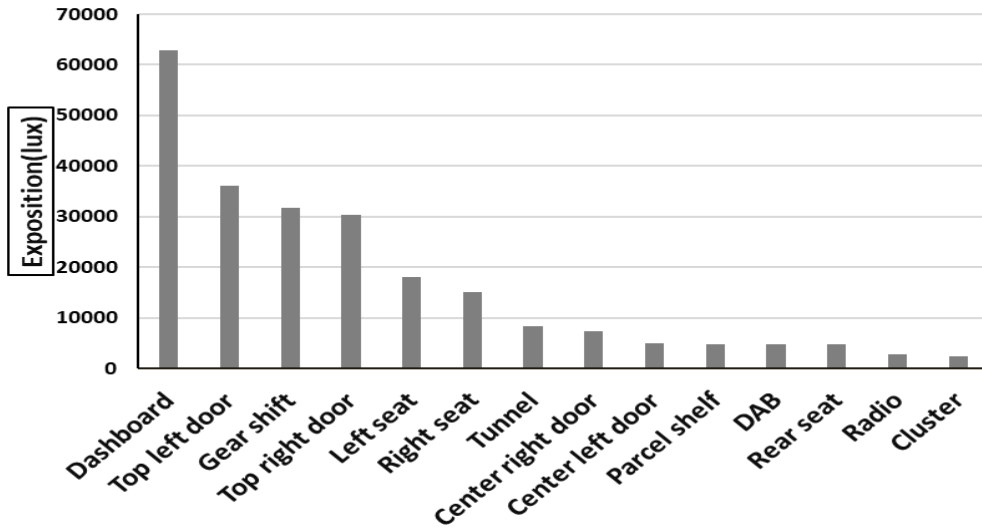
Figure A.4. Average daylight illuminance weighted to irradiance (lux)-Segment B

Bibliography

1 . V Wong, K., & A Paddon, P. (2014). Nanotechnology impact on the automotive industry. Recent patents on nanotechnology, 8(3), 181-199.

2 . Shamsundara, B. V., Mannikar, A. V., & Shridhar, T. N. (2011). Study on Polymer Degradation due to Weathering and its Effect on Vehicle Safety (No. 2011-26-0097). SAE Technical Paper

3 . Mayne, N. Plastics-A material choice in the automotive industries. *Association of plastics manufactures in Europe, Technical paper*

4 . Chandra, R., & Saini, R. (1990). New developments in the degradation, stabilization, and sensitization of poly (methyl methacrylate). *Journal of Macromolecular Science—Reviews in Macromolecular Chemistry and Physics*, *30*(2), 155-208

5 . Iannuzzi, G., Mattsson, B., & Rigdahl, M. (2013). Color changes due to thermal ageing and artificial weathering of pigmented and textured ABS. *Polymer Engineering & Science*, *53*(8), 1687-1695.

6 . FORMULATION OF INDIA SPECIFIC WEATHERING CYCLE REQUIRED FOR POLYMER TEST

7 . NEW Q-FOG CRH CYCLIC CORROSION TESTER WITH RELATIVE HUMIDITY CONTRO

8 . Zito, S., Castel, T., Richard, Y., Rega, M., & Bois, B. (2020). Optimization of a leaf wetness duration model. *Agricultural and Forest Meteorology*, *291*, 108087

9 . Gok, A., Ngendahimana, D. K., Fagerholm, C. L., French, R. H., Sun, J., & Bruckman, L. S. (2017). Predictive models of poly (ethylene-terephthalate) film degradation under multi-factor accelerated weathering exposures. *PloS one*, *12*(5), e0177614

10 . Krzymien, M. E. (1997, April). PVC photo-oxidative degradation: Identification of volatiles. In *Macromolecular Symposia* (Vol. 115, No. 1, pp. 27-40). Basel: Hüthig & Wepf Verlag

11 . Hollande, S., & Laurent, J. L. (1998). Weight loss during different weathering tests of industrial thermoplastic elastomer polyurethane-coated fabrics. *Polymer degradation and stability*, *62*(3), 501-505

12 . SAE, J. (1885). Accelerated Exposure of Automotive Interior Trim Components Using a Controlled Irradiance Water Cooled Xenon-Arc Apparatus, 1993 KJ/m2 irradiance, borosilicate filter. *Society of Automotive Engineers*

13 . Ram, A., Zilber, O., & Kenig, S. (1985). Life expectation of polycarbonate. *Polymer Engineering & Science*, *25*(9), 535-540

14 . Ram, A., Zilber, O., & Kenig, S. (1985). Residual stresses and toughness of polycarbonate exposed to environmental conditions. *Polymer Engineering & Science*, *25*(9), 577-581

15 . Sherman, E. S., Ram, A., & Kenig, S. (1982). Tensile failure of weathered polycarbonate. *Polymer Engineering & Science*, *22*(8), 457-465.

16 . Tjandraatmadja, G. F., Burn, L. S., & Jollands, M. C. (2002). Evaluation of commercial polycarbonate optical properties after QUV-A radiation—the role of humidity in photodegradation. *Polymer degradation and stability*, *78*(3), 435-448

17 . Shamsundara, B. V., Mannikar, A. V., & Shridhar, T. N. (2011). Study on Polymer Degradation due to Weathering and its Effect on Vehicle Safety (No. 2011-26-0097). SAE Technical Paper

18 . Tocháček, J., & Vrátníčková, Z. (2014). Polymer life-time prediction: The role of temperature in UV accelerated ageing of polypropylene and its copolymers. *Polymer Testing*, *36*, 82-87

19 . Miller, D. C., Carloni, J. D., Johnson, D. K., Pankow, J. W., Gjersing, E. L., To, B., ... & Kurtz, S. R. (2013). An investigation of the changes in poly (methyl methacrylate) specimens after exposure to ultra-violet light, heat, and humidity. *Solar energy materials and solar cells*, *111*, 165-180

20 . Shioda, T. (2011, September). UV-accelerated test based on analysis of field-exposed PV modules. In *Reliability of Photovoltaic Cells, Modules, Components, and Systems IV* (Vol. 8112, p. 81120I). International Society for Optics and Photonics

21 . Poisson, C., Hervais, V., Lacrampe, M. F., & Krawczak, P. (2006). Optimization of PE/binder/PA extrusion blow-molded films. II. Adhesion properties improvement using binder/EVA blends. *Journal of applied polymer science*, *101*(1), 118-127

22 . Awaja, F., Gilbert, M., Kelly, G., Fox, B., & Pigram, P. J. (2009). Adhesion of polymers. *Progress in polymer science*, *34*(9), 948-968

23 . Hochrein, T., & Alig, I. (2011). Prozessmesstechnik in der Kunststoffaufbereitung (process measurement techniques for plastics compounding). *Vogel-Verlag, Wuerzburg*

24 . Botos, J., Murail, N., Heidemeyer, P., Kretschmer, K., Ulmer, B., Zentgraf, T., ... & Hochrein, T. (2014, May). Color measurement of plastics-From compounding via pelletizing, up to injection molding and extrusion. In *AIP Conference Proceedings* (Vol. 1593, No. 1, pp. 16-19). American Institute of Physics

25 . Botos, J., Murail, N., Heidemeyer, P., Kretschmer, K., Ulmer, B., Zentgraf, T., ... & Hochrein, T. (2014, May). Color measurement of plastics-From compounding via pelletizing, up to injection molding and extrusion. In *AIP Conference Proceedings* (Vol. 1593, No. 1, pp. 16-19). American Institute of Physics.

26 . A. Chrisment in Editions 3C Conseil, Paris, 1993

27 . Gok, A., Gordon, D. A., Wang, M., French, R. H., & Bruckman, L. S. (2019). Degradation Science and Pathways in PV Systems. In *Durability and Reliability of Polymers and Other Materials in Photovoltaic Modules* (pp. 47-93). William Andrew Publishing

28 . Andreassen, E., Larsen, Å., Nord-Varhaug, K., Skar, M., & Øysæd, H. (2002). Haze of polyethylene films—effects of material parameters and clarifying agents. *Polymer Engineering & Science*, *42*(5), 1082-1097.

29 . Sun, Z., Fan, H., Chen, Y., & Huang, J. (2018). Synthesis of self-matting waterborne polyurethane coatings with excellent transmittance. *Polymer International*, *67*(1), 78-84.][

Vessot, K., Messier, P., Hyde, J. M., & Brown, C. A. (2015). Correlation between gloss reflectance and surface texture in photographic paper. *Scanning*, *37*(3), 204-217

30 . Yong, Q., Nian, F., Liao, B., Guo, Y., Huang, L., Wang, L., & Pang, H. (2017). Synthesis and surface analysis of self-matt coating based on waterborne polyurethane resin and study on the matt mechanism. *Polymer Bulletin*, *74*(4), 1061-1076.

31 . Elton, N. J., & Day, J. C. C. (2009). A reflectometer for the combined measurement of refractive index, microroughness, macroroughness and gloss of low-extinction surfaces. *Measurement Science and Technology*, *20*(2), 025309

32 . Yong, Q., Chang, J., Liu, Q., Jiang, F., Wei, D., & Li, H. (2020). Matt Polyurethane Coating: Correlation of Surface Roughness on Measurement Length and Gloss. *Polymers*, *12*(2), 326

33 . Iannuzzi, G., Mattsson, B., & Rigdahl, M. (2013). Color changes due to thermal ageing and artificial weathering of pigmented and textured ABS. *Polymer Engineering & Science*, *53*(8), 1687-1695

34 . Yong, Q., Chang, J., Liu, Q., Jiang, F., Wei, D., & Li, H. (2020). Matt Polyurethane Coating: Correlation of Surface Roughness on Measurement Length and Gloss. *Polymers*, *12*(2), 326

35 . Juuti, M., Prykäri, T., Alarousu, E., Koivula, H., Myllys, M., Lähteelä, A., ... & Peiponen, K. E. (2007). Detection of local specular gloss and surface roughness from black prints. *Colloids and Surfaces A: Physicochemical and Engineering Aspects*, *299*(1-3), 101-108

36 . Yong, Q., & Liang, C. (2019). Synthesis of an Aqueous Self-Matting Acrylic Resin with Low Gloss and High Transparency via Controlling Surface Morphology. *Polymers*, *11*(2), 322

37 . Cawthorne, J. E., Joyce, M., & Fleming, D. (2003). Use of a chemically modified clay as a replacement for silica in matte coated ink-jet papers. *Journal of Coatings Technology*, *75*(937), 75-81

38 . Ou, J., Zhang, M., Liu, H., Zhang, L., & Pang, H. (2015). Matting films prepared from waterborne acrylic/micro-SiO2 blends. *Journal of Applied Polymer Science*, *132*(13)

39 . Bauer, F., Decker, U., Czihal, K., Mehnert, R., Riedel, C., Riemschneider, M., ... & Buchmeiser, M. R. (2009). UV curing and matting of acrylate nanocomposite coatings by 172 nm excimer irradiation. *Progress in Organic Coatings*, *64*(4), 474-481

40 . Lin, H., Wang, Y., Gan, Y., Hou, H., Yin, J., & Jiang, X. (2015). Simultaneous formation of a self-wrinkled surface and silver nanoparticles on a functional photocuring coating. *Langmuir*, *31*(43), 11800-11808

41 . Tjandraatmadja, G. F., Burn, L. S., & Jollands, M. C. (2002). Evaluation of commercial polycarbonate optical properties after QUV-A radiation—the role of humidity in photodegradation. *Polymer degradation and stability*, *78*(3), 435-448

42 . De Chiffre, L., Lonardo, P., Trumpold, H., Lucca, D. A., Goch, G., Brown, C. A., ... & Hansen, H. N. (2000). Quantitative characterisation of surface texture. *CIRP Annals*, *49*(2), 635-652

43 . Blateyron, F. (2013). The areal field parameters. In *Characterisation of areal surface texture* (pp. 15-43). Springer, Berlin, Heidelberg

44 . ISO, I. (2012). 25178-2: 2012—Geometrical Product Specifications (GPS)—Surface Texture: Areal—Part 2: Terms, Definitions and Surface Texture Parameters. *International Standards Organization: Geneva, Switzerland*

45 . Downey, T. (2016). *A computational analysis of the application of skewness and kurtosis to corrugated and abraded surfaces* (Doctoral dissertation, Memorial University of Newfoundland)

46 . Blateyron, F. (2013). The areal field parameters. In *Characterisation of areal surface texture* (pp. 15-43). Springer, Berlin, Heidelberg

47 . Nair, A., Sharma, P., Sharma, V., & Diwan, P. K. (2020). Effect of UV-irradiation on the optical properties of transparent PET polymeric foils. *Materials Today: Proceedings*, *21*, 2105-2111

48 . Gok, A., Ngendahimana, D. K., Fagerholm, C. L., French, R. H., Sun, J., & Bruckman, L. S. (2017). Predictive models of poly (ethylene-terephthalate) film degradation under multi-factor accelerated weathering exposures. *PloS one*, *12*(5), e0177614

49 . Standard, A. S. T. M. (2012). G173-03-Standard Tables for Reference Solar Spectral Irradiances: Direct Normal and Hemispherical on 37 Tilted Surface. *Ann. Book of ASTM Standards 2003*, *14*, 1-20.

50 . ASTM G154-16, Standard Practice for Operating Fluorescent Ultraviolet (UV) Lamp Apparatus for Exposure of Nonmetallic Materials. West Conshohocken, PA: ASTM International; 2016.

51 . Gok, A., Ngendahimana, D. K., Fagerholm, C. L., French, R. H., Sun, J., & Bruckman, L. S. (2017). Predictive models of poly (ethylene-terephthalate) film degradation under multi-factor accelerated weathering exposures. *PloS one*, *12*(5), e0177614

52 . J.F. Rabek, Polymer Photodegradation - Mechanisms and Experimental Methods, Chapman & Hall, London, UK (1995).

53 . J.G. Borkia and S. Schlick, Polymers, 43, 3239 (2002).

54 . R.M. Santos, G.L. Botelho, and A.V. Machado, J. Appl. Polym. Sci., 116, 2005 (2010)

55 . J.F. Rabek, ''Photochemical Aspects of Degradation of Polymers,'' Polymer Photodegradation - Mechanisms and Experimental Methods, Chapman & Hall, London, UK (1995)

56 . B.E. Tiganis, L.S. Burn, P. Davis, and A.J. Hill, Polym. Degrad. Stab., 76, 425 (2002).

57 . J. Shimada and K. Kabuki, J. Appl. Polym. Sci., 12, 655 (1968).

58 . J. Shimada and K. Kabuki, J. Appl. Polym. Sci., 12, 671 (1968).

59 . J.F. Rabek, ''Photodegradation and Photo-oxidative Degra- dation of Homochain Polymers,'' Polymer Photodegradation - Mechanisms and Experimental Methods, Chapman & Hall, London, UK (1995).

60 . Iannuzzi, G., Mattsson, B., & Rigdahl, M. (2013). Color changes due to thermal ageing and artificial weathering of pigmented and textured ABS. Polymer Engineering & Science, 53(8), 1687-1695

61 . Shimada, J., & Kabuki, K. (1968). The mechanism of oxidative degradation of ABS resin. Part I. The mechanism of thermooxidative degradation. *Journal of Applied Polymer Science*, *12*(4), 655-669

62 . Boldizar, A., & Möller, K. (2003). Degradation of ABS during repeated processing and accelerated ageing. *Polymer degradation and stability*, *81*(2), 359-366.

63 . Ashby, M. F., & Cebon, D. (1993). Materials selection in mechanical design. *Le Journal de Physique IV*, *3*(C7), C7-1

64 . Altuglas International Plexiglas UF-3 UF-4 and UF-5 sheets, 2006-11-17 at the Wayback Machine. Plexiglas.com. Retrieved 2012-05-09.

65 . *Andrei, D., Ana-Maria, A., Claudiu, B., Oana, C., & Liviu, U. (2018). OBTAINING COMPOSITE MATERIALS OF THE POLYMER-ALUMINIUM TYPE BY GLUING USING BICOMPONENT ADHESIVES. International Multidisciplinary Scientific GeoConference: SGEM, 18(6.1), 355-362*

66 . Wypych, G. (2016). *Handbook of polymers*. Elsevier

67 . Data from Torikai, A; Hasegawa, H, Polym. Deg. Stab., 61, 2, 361-4, 1998.

68 . Wypych, G. (2016). *Handbook of polymers*. Elsevier

69 . Miller, D. C., Gedvilas, L. M., To, B., Kennedy, C. E., & Kurtz, S. R. (2010, August). Durability of poly (methyl methacrylate) lenses used in concentrating photovoltaic modules. In *Reliability of Photovoltaic Cells, Modules, Components, and Systems III* (Vol. 7773, p. 777303). International Society for Optics and Photonics

70 . Miller, D. C., Carloni, J. D., Johnson, D. K., Pankow, J. W., Gjersing, E. L., To, B., ... & Kurtz, S. R. (2013). An investigation of the changes in poly (methyl methacrylate) specimens after exposure to ultra-violet light, heat, and humidity. *Solar energy materials and solar cells*, *111*, 165-180.

71 . Seubert, C., Nietering, K., Nichols, M., Wykoff, R., & Bollin, S. (2012). An overview of the scratch resistance of automotive coatings: exterior clearcoats and polycarbonate hardcoats. *Coatings*, *2*(4), 221-234

72 . Pickett, J. E., Gibson, D. A., & Gardner, M. M. (2008). Effects of irradiation conditions on the weathering of engineering thermoplastics. *Polymer Degradation and Stability*, *93*(8), 1597-1606.

73 . Brennan P, Fedor C. Sunlight, UV, and accelerated weathering. Surface Coatings Australia 1988:7–11

74 . Tjandraatmadja, G. F., Burn, L. S., & Jollands, M. C. (2002). Evaluation of commercial polycarbonate optical properties after QUV-A radiation—the role of humidity in photodegradation. *Polymer degradation and stability*, *78*(3), 435-448

75 . American Society for Testing and Materials. Test method for specular gloss of plastic films and solid plastics, vol. 8.02. ASTM D2457–97. Philadelphia: ASTM; 1997

76 . Trajkovska-Petkoska, A., & Nasov, I. (2014). Surface engineering of polymers: Case study: PVD coatings on polymers. *Zaštita materijala*, *55*(1), 3-10.

77 . Martin, P. M. (2010). Thin Film Coatings, III-rd Ed.

78 . Joshi, M., & Butola, B. S. (2013). Application technologies for coating, lamination and finishing of technical textiles. In *Advances in the dyeing and finishing of technical textiles* (pp. 355-411). Woodhead Publishing.

79 . Guerrero, H., Rosa, G., Morales, M. P., Del Monte, F., Moreno, E. M., Levy, D., ... & Serna, C. J. (1997). Faraday rotation in magnetic γ-Fe 2 O 3/SiO 2 nanocomposites. *Applied physics letters*, *71*(18), 2698-2700

80 . Vu-Khanh, T., Sanschagrin, B., & Fisa, B. (1985). Fracture of mica-reinforced polypropylene: Mica concentration effect. *Polymer composites*, *6*(4), 249-260.

81 . Meeten, G. H. (1986). Optical properties of polymers. *Elsevier Applied Science Publishers Ltd, Crown House, Linton Road, Barking, Essex IG 11 8 JU, UK, 1986*

82 . Zhou, R. J., & Burkhart, T. (2010). Optical properties of particle-filled polycarbonate, polystyrene, and poly (methyl methacrylate) composites. *Journal of applied polymer science*, *115*(3), 1866-1872.]

83 . Seubert, C., Nietering, K., Nichols, M., Wykoff, R., & Bollin, S. (2012). An overview of the scratch resistance of automotive coatings: exterior clearcoats and polycarbonate hardcoats. *Coatings*, *2*(4), 221-234